Lawrence Berkeley National Laboratory
LBL Publications

Title
Experimental studies of the flow of ferrofluid in porous media

Permalink
https://escholarship.org/uc/item/6jj559gx

Author
Borglin, Sharon

Publication Date
1998-08-01

ERNEST ORLANDO LAWRENCE BERKELEY NATIONAL LABORATORY

Experimental Studies of Magnetically Driven Flow of Ferrofluids in Porous Media

Sharon E. Borglin, George J. Moridis, and Curtis M. Oldenburg

Earth Sciences Division

August 1998

DISCLAIMER

Experimental Studies of Magnetically Driven Flow
of Ferrofluids in Porous Media

Sharon E. Borglin, George J. Moridis, and Curtis M. Oldenburg

Earth Sciences Division

Lawrence Berkeley National Laboratory

University of California

Berkeley, California 94720

August 1998

Abstract

This report presents experimental results of the flow of ferrofluids in porous media to investigate the potential for precisely controlling fluid emplacement in porous media using magnetic fields. Ferrofluids are colloidal suspensions of magnetic particles stabilized in various carrier liquids. In the presence of an external magnetic field, the ferrofluid becomes magnetized as the particles align with the magnetic field. In the presence of a gradient in the magnetic field strength, a magnetic body force is produced on the ferrofluid. Potential applications of ferrofluids to subsurface contamination problems include magnetic guidance of reactants to contaminated target zones in the subsurface for *in situ* treatment or emplacement of containment barriers. Prior to the design of large scale experiments or field demonstrations, an understanding of the behavior of ferrofluids in porous media is required. Laboratory experiments of magnetically induced ferrofluid flow in porous media in this report demonstrate the potential for mobilizing ferrofluid and controlling fluid emplacement through control of the external magnetic field. The pressures measured in ferrofluid due to the attraction of ferrofluid to a permanent magnet agree well with calculated values. The results show that a predictable pressure gradient is produced in the fluid which is strong near the magnet and drops off quickly with distance. This pressure gradient drives the fluid through sand without significant loss of ferrofluid strength due to filtration or dilution. Flow visualization experiments of ferrofluid in water-filled horizontal Hele-Shaw cells demonstrate that ferrofluid obtains a consistent final arc-shaped configuration around the magnet regardless of initial configuration or flow path toward the magnet. Analogous experiments in actual porous media showed similar features and confirm the ability of ferrofluid to move through porous media by magnetic forces. The experiments reported on here support the concept of using ferrofluids to aid in the precise placement of fluids in porous media in laboratory or subsurface applications to aid in the precise placement of fluids in the subsurface.

Nomenclature

B	induced field	T
B_r	residual magnetic induction of permanent magnet	T
H	external magnetic field	A/m
H_x	x component of the magnetic field	A/m
M	magnetization	A/m
$\overline{M}$	field-averaged magnetization	A/m
M_n	magnetization normal to the surface	A/m
p_o	ambient atmospheric pressure	Pa
p_n	normal pressure	Pa
p_c	capillary pressure	Pa
p_G	magnetopressure (gauge)	Pa
h	height of deformation of the surface of a ferrofluid	m
g	gravitational acceleration	m/s^2
g_m	magnetic gravity	m/s^2
$2a$	height of a permanent magnet	m
$2b$	width of a permanent magnet	m
L_o	length of a permanent magnet	m
x	distance along centerline of a magnetic pole	m
y	distance perpendicular to a magnetic pole	m
z	distance perpendicular to a magnetic pole	m
K	hydraulic conductivity	m/s
k	permeability of a porous medium	m^2
a	gap width of Hele-Shaw cell	m
u_1	parameter describing magnetic effects	N/kg
u_2	parameter describing magnetic effects	N/kg
D_{10}	10th percentile diameter of a article size distribution	m

μ_m	magnetic permeability	*Tm/A*
μ_{mo}	magnetic permeability of free space	*Tm/A*
μ	viscosity	*Pa·s*
σ	interfacial tension	*N/m*
$\mathscr{H}$	arithmetic mean curvature	*1/m*
ρ	density	*kg/m³*

1. Introduction

The purpose this report is to gain an understanding of the behavior of ferrofluids in porous media and to evaluate whether they can be precisely controlled and directed in the subsurface using magnetic fields. Ferrofluids are stable colloidal suspensions of magnetic particles stabilized in various carrier liquids (Raj and Moskowitz, 1990). The solid, magnetic, single-domain particles are small (with an average diameter of 10 nm) and are covered with a molecular layer of a dispersant. Thermal agitation due to Brownian motion keeps the particles suspended, while the dispersant coating prevents the particles from agglomerating. The ferrofluid is a stable liquid. An external magnetic field cannot segregate the magnetic particles out of the carrier liquid, i.e., the concentration of the particles in the pure ferrofluid remains spatially and temporally constant regardless of the strength of the external field. Consequently, ferrofluids behave like a homogeneous single-phase fluid when flowing under the influence of a magnetic field. This attribute is responsible for the unique ability of ferrofluids to be manipulated in virtually any fashion, defying gravitational or viscous forces in response to external magnetic fields. Therefore, ferrofluids can be made to flow in a desired direction and move precisely without any direct physical contact (Chorney and Mraz, 1992).

4

To achieve more precise control of the placement of substances in the subsurface, these unique fluids may be stabilized with various carrier liquids, including those with environmental remediation applications. The potential uses of ferrofluids have been discussed by Moridis and Oldenburg (1998), and include using magnetic fields for flow control for guidance of reactants to contaminated target zones in the subsurface for *in situ* treatment, sealing of steel underground storage tanks, and emplacement of barrier liquids (low-viscosity permeation grouts).

Understanding the basic principles controlling and limiting the use of this technology for subsurface guidance applications is necessary to evaluate the potential uses of ferrofluids. This report details experiments which investigate the behavior of ferrofluids in porous media. The force created in a ferrofluid by an external magnetic field is quantified by measuring the "magnetopressure" (Moridis and Oldenburg, 1998), i.e., the pressure induced in the ferrofluid by a magnetic field. Also investigated is the effect of ferrofluid-particle interaction on the strength of ferrofluids as they pass through porous media, and the effect of the magnetic field on the water miscibility and segregation of diluted ferrofluid. This evaluation also includes flow visualization of ferrofluid migration in Hele-Shaw cells and in sand.

These experiments demonstrate that the ferrofluid can be effectively directed through porous media using magnetic fields, although the length scales in which this driving force is limited to the order of 1 m. The limitation in the length scales is derived from the rapid decline in the strength of the magnetic field with distance. An important observation is, however, the end configuration of the ferrofluid is predictable and is independent of the initial configuration of injection. Ferrofluid technology would therefore produce a powerful and controllable subsurface guidance force over these limited distances.

2. Magnetic Properties of Ferrofluids

In the absence of a magnetic field, the ferrofluid particles are randomly oriented, the fluid has no net magnetization, and there is no long-range order between the colloidal ferrofluid particles. In the presence of an external magnetic field, ferrofluid particles align with the field and the ferrofluid becomes magnetized. Ferrofluids behave as soft magnetic materials, i.e., small changes in the field result in substantial magnetization changes, and they do not exhibit hysteresis.

The study of ferrofluids involves traditional ferromagnetic concepts. The relationship between the induced field, B, the external magnetic field, H, and the intensity of magnetization, M, of a ferrofluid is given by

$$B = \mu_m (H + M) \tag{1}$$

where μ_m is the magnetic permeability of the medium. For free space (i.e., air), $\mu_m = \mu_{mo}$, which has the value of $4\pi \times 10^{-7}$ T m/A (Tesla-meter/Ampere). In soft magnets, such as ferrofluid, M and H are aligned which allows us to equate the vector quantities M and H with the magnitudes M and H in relations such as Equation 1. The intrinsic magnetization curve of a commercially available ferrofluid, EMG 805[TM], (Ferrofluidics Corp., Nashua, N. H.) is shown in Figure 1.

A number of fundamental equations relating ferrofluid forces to magnetic field have be presented by Rosensweig (1995). For example, the force exerted on a ferrofluid in response to an external field is given by the equation

$$F = \mu_m M \nabla H \; , \tag{2}$$

where M and H are the magnitudes of the magnetization and the magnetic field and are given in A/m (Ampere/meter). The balance of forces acting on a fluid is described by the ferrohydrodynamic Bernoulli equation,

$$p_o + p_n + p_c + \rho\frac{v^2}{2} + \rho gh - \mu_m\overline{M}H = cons \tan t \tag{3}$$

where $\overline{M}$ is the field-average magnetization given by

$$\overline{M} = \frac{1}{H}\int_0^H MdH, \tag{4}$$

and p_o is the ambient atmospheric pressure. The normal and capillary pressures, p_n and p_c, respectively, are given by the expressions,

$$p_n = \frac{1}{2}\mu_m M_n^2 \tag{5}$$

$$p_c = 2\mathcal{H}\sigma \tag{6}$$

where M_n is the magnetization normal to the surface of the fluid, $\mathcal{H}$ is the arithmetic mean curvature (equal to 1/R for a sphere and 1/2R for a cylinder), and σ is the interfacial tension.

These equations can be used to estimate the deformation of a ferrofluid in a magnetic field. For example, to describe the change in surface elevation of a ferrofluid in a magnetic field, the form of the ferrohydrodynamic Bernoulli equation is given by

$$\Delta h = \frac{1}{\rho g}\left(\mu_m\overline{M}H\right) \tag{7}$$

where h is the height of deformation, ρ is the density of the ferrofluid, and g is gravitational acceleration. Full derivation and further details of the above equations can be found in Rosensweig (1985).

3. Materials

In this study we used two ferrofluids, EMG 805™ (FF1) and EMG-C™ (FF2) (Ferrofluidics Corporation, Nashua, N.H.) and a variety of tubes, flow cells, and magnets. Table 1 summarizes the physical properties of the two fluids. Both of these ferrofluids used water as the carrier liquid. The larger magnetite concentration in FF2 results in a higher saturation magnetization for this fluid. The stabilization of the magnetic particles is achieved by means of a water-soluble dispersant (surfactant). To avoid potential interaction between the negatively-charged soil particles and the ferrofluid, both ferrofluids were selected with anionic dispersants and neutral pH. All concentrations given in Table 1 are by volume.

The porous media used in the experiments are described in Table 2. Monterey #60 sand (RMC Lonestar, Pleasanton, California), OK-1 silica sand (Pyro Minerals, Oakland, California), and Unimin 30/40 mesh silica sand (Unimin Corp., Le Sueur, MN), hereafter referred to as S2, S4, and S3, are commercially available. The NTS soil, hereafter referred to as S1, was obtained from a surface grab at the Nevada Test Site, and was sieved through a 2 mm sieve to remove larger grains.

Neodymium iron boron (NdFeB) permanent magnets were used to create the magnetic fields in the experiments (Table 3). For ease of differentiation, the magnets are referred to as PM1 (Pacific Century Enterprises, Centreville, VA) and PM2 (courtesy of R. Schlueter, Advanced Light Source, LBNL). As shown in Figure 2, The terms *2a* and *2b* refer to the height and width of the rectangular permanent magnets. Five units of the PM1 magnets were often used in a stacked arrangement, which was equivalent to a single magnet with length (L_o) = 0.127 m.

The 3-dimensional magnetic field created by a rectangular permanent magnet (such as the NdFeB blocks) can be described by the analytical expressions of McCaig and Clegg, (1987). The equation for the x component of the magnetic field simplifies to

$$H_x = \frac{B_r}{\pi\mu_m}\left[tan^{-1}\left(\frac{ab}{x(a^2+b^2+x^2)^{\frac{1}{2}}}\right) - tan^{-1}\left(\frac{ab}{(x+L_o)(a^2+b^2+(x+L_o)^2)^{\frac{1}{2}}}\right)\right] \qquad (8)$$

where x is the position along the centerline of the magnet (see Figure 2). B_r, the residual induction of the permanent magnets, represents the maximum magnetic flux output from the given magnet.

Equation (8) was verified for the PM1 and PM2 magnets by measuring the magnetic field using a DTM 141-G Group 3 Teslameter equipped with a LPT-141 probe (Group 3 Technology Ltd., Auckland, New Zealand). Figure 3 shows excellent agreement between measurements and analytical predictions of the field created by five PM1 magnets.

4. Experimental Studies

The experiments discussed in this section were designed to characterize the flow of ferrofluid through porous media, and include (1) initial verification of the ferrohydrodynamic Bernoulli equation, (2) filtration effects, (3) measurement of magnetopressure, (4) magnetically induced flow through horizontal and vertical Hele-Shaw cells, and (5) magnetically induced ferrofluid flow through porous media.

4.1. Initial verification of Ferrohydrodynamic Bernoulli equation

Preliminary experiments were designed to verify equation (7) for the ferrofluid and magnets used in the experiments. The PM2 magnet was used to observe vertical deformation of a horizontal pool of FF1 fluid. The magnet was oriented so that the x-axis was perpendicular to the free surface of the ferrofluid pool, and was then lowered until the surface of the ferrofluid was visibly deformed (on the order of 1 mm). This occurred when the magnet-ferrofluid gap was 0.08 m from the original surface. At this distance, equation (8) predicts a field of 4×10^4 A/m The magnetization of the ferrofluid at this field strength (as determined by the B-H curve in Figure 1) is 9×10^3 A/m. Using these values, equation (7) results in a predicted deformation of 2 mm, which is comparable with the observed deformation.

4.2. Filtration Effects

Moridis and Oldenburg (1998) indicated that ferrofluids are not affected by surface or straining filtration due to their small particle size, which averages 10 nm and does not exceed 20 nm (Nunes and Yu, 1987). However, filtration removes particles smaller than pore throats by physical-chemical filtration (Moridis and Oldenburg, 1998), which could adversely affect their properties and performance in subsurface targeting applications. To determine the magnitude of physical-chemical filtration, ferrofluids were eluted through columns filled with porous media.

The porous media used in this experiment were S1, S2, and S4, the properties of which are summarized in Table 2. The tests in this set of experiments included flow and filtration through: (1) water-saturated S2, (2) water-saturated S1, (3) water-saturated S4, (4) partially saturated S4 and (5) dry S4.

The apparatus used (shown in Figure 4) consisted of a vertical, acrylic, sand-filled tube 1.0 cm in diameter and 15 cm long filled with the porous medium and connected to a syringe pump which injects liquid into the bottom of the column. For experiments (1) through (4), the column was initially saturated by injecting water at a rate of 0.5 ml/min until no gas bubbles were visually in the column.

After saturation with water, FF1 ferrofluid was injected directly into the water-saturated medium at the bottom of the column using the syringe pump. In the S2 and S4 sand tests, the injection rate of ferrofluid was 0.5 ml/hr. Due to the lower permeability of the S1 soil, the injection rate of both water (for the initial saturation) and ferrofluid was decreased to 0.25 ml/hr to limit back pressure on the syringe pump. In the tests with the partially saturated S4 sand, the column was drained after water saturation for 14 hours prior to ferrofluid injection. In the test with the dry S4 sand, the apparatus was cleaned, dried and filled with S4 sand prior to the test.

Effluent samples were collected every minute for the S4 sand and the S2 sand and every two minutes for S1 soil. The effluent samples from the S2 and S4 saturated sands were analyzed for magnetic susceptibility using a Magnetic Susceptibility Bridge Model MS-3 (Geophysical Specialties Company, Minneapolis, Minnesota). The samples from the S1, the unsaturated S4 column, and the dry S4 column were analyzed for ferrofluid concentration using a HACH Model DR/2000 spectrometer (Loveland, CO), which was calibrated using a ferrofluid stock solution. Both of these methods are capable of determining the concentration of magnetite in the ferrofluid over the range of interest.

The effluent measurements from the three saturated porous media tests are shown in Figure 5. None of the media exhibited significant retention of the ferrofluid. The time required to

achieve full ferrofluid concentration ranged from two pore volumes for the S2 sand to 5 pore volumes for the S4 and S1 saturated media.

Figure 6 shows the effluent concentrations for the dry, partially saturated, and fully saturated S4 sands. The number of pore volumes required to reach full ferrofluid concentration ranges from less than one pore volume for the dry S4 sand to four pore volumes for the S4 saturated sand. Therefore, the concentration of the eluted ferrofluid decreases with the amount of water in the sand. This suggests that dilution by pore water, rather than filtration, is the dominant factor in the decreasing of ferrofluid strength. In this system, the dispersants in the ferrofluid effectively flush the system and displace the water present in the column. This is evident in the case of the dry S1 sand, where the fluid flushed out the trace of residual water in the system, causing the observed delay to reach full ferrofluid strength.

The results were analyzed for filtration effects by models described by Lerk (1967), Herzig et. al. (1970), Dieulin (1982), and Ives (1975), but all failed to predict the observed data. Modeling of the filtration of ferrofluid by conventional solute transport equations is difficult because the density effects make the analysis strongly non-linear. Some unidentified physical-chemical sorption processes may occur in the soils investigated in the present study. However, only very minor effects due to this mechanism are observed.

4.3. MAGNETICALLY-CONTROLLED SEGREGATION AND SOLUBILITY

A balance among several forces is required to maintain a stable ferrofluid.. These forces include (1) magnetic dipole-dipole interaction; (2) van der Waals interaction; (3) dipole-magnetic field interaction; and (4) steric repulsion (Berkovski, 1996). The forces are controlled during

manufacture by the relative amounts of magnetite, surfactant and water in the composition of a given ferrofluid. The stability of the fluid may change during flow through natural porous media due to dilution, as additional water is incorporated into the moving front of a fully-miscible ferrofluid. To investigate the behavior of ferrofluids as affected by miscibility, two experiments were designed. The first experiment investigated potential segregation of ferrofluid from a diluted ferrofluid-water mixture under the influence of a magnetic field. The second experiment investigated potential inhibition of miscibility of an otherwise fully water-miscible ferrofluid when under the influence of a magnetic field.

4.3.1. Magnetic segregation.

FF1 ferrofluid was diluted with deionized water to 16 % of its original concentration. Two 20 ml vials were filled with the diluted fluid to a depth of 4.2 cm (volume = 18 ml). One vial was placed on the north pole of the five stacked PM1 magnets, while the other was not subjected to a magnetic field. The concentration of the fluid was monitored at the liquid free surface (4.2 cm from magnet and vial bottom), 2 cm from the bottom of the vial, 1 cm from the bottom of the vial, and at the bottom of the vial. Concentrations were measured by removing small aliquots of the fluid which were analyzed using the HACH spectrophotometer and reported as percentage of pure fluid. The evolution of concentration profiles over time at these four locations is shown in Figure 7.

Figure 7A shows concentration changes for the vial placed on the magnet. The concentration of fluid at the 4.2 cm (at the top of the fluid), 2 and 1 cm from the magnet ranges from 2 to 4 %, while the concentration at the bottom of the vial is nearly 100 % after 0.25 hours.

The vial without a magnetic field is shown in Figure 7B. The concentration in this vial did not change significantly over time. After 48 hours, the concentration in this vial with no magnetic field varied from 15.9 % at the fluid surface to 17 % at the bottom of the vial. This small difference is attributed to gravitational settling.

Two additional sets of tests were performed on vials containing diluted FF1 ferrofluid. In the first set, three vials containing a 1:1 ferrofluid dilution to a height of 2 cm (volume 2 ml) were placed at distances of 0, 1, and 2 cm from the 5 stacked PM1 magnets. After 24 hours, the ferrofluid in all three vials was determined spectrophotometrically to have a ferrofluid concentration in the top layer of less than 1% and a bottom layer concentration of 100%.

The second set of tests, shown in Figure 8, consisted of two vials containing 50 % and 33 % dilutions of FF1 ferrofluid in water, respectively. The vial containing 50 % ferrofluid (1:1 dilution) was filled to a height of 2 cm (volume 2 ml) and the vial containing 30 % ferrofluid (1:2 dilution) was filled to a height of 3 cm (volume 3 ml). The vials were then covered and placed directly on the 5 stacked PM1 magnets for 30 days. At the end of this period, there was no detectable ferrofluid in the overlying water, and the concentration in the bottom of the vial was measured to be 100 % pure ferrofluid using the HACH spectrometer. In addition, the total height of the liquid in the 1:1 vial was 2 cm, and the height to the dark-light interface was 1 cm. The total height of the 1:2 diluted ferrofluid was 2.5 cm, and the height of the ferrofluid was 1 cm. It is suspected that some evaporation occurred in this vial due to incomplete sealing. The separation observed in these vials implies that the solution was volumetrically separated. Vials not influenced by a magnetic field (see example in Figure 8D) did not separate after 30 days.

These experiments indicate that the original ferrofluid can be recovered from a diluted ferrofluid using a magnetic field. The recovered ferrofluid has the same concentration of magnetite as the original sample. In porous media, if ferrofluid becomes diluted during transport or injection, subsequent addition of a magnetic field and field gradient would serve to separate the ferrofluid from the surrounding pore water. If the carrier liquid were to contain barrier forming compounds, this phenomenon is a barrier liquid, this would be advantageous, otherwise dilution of the barrier liquid by ferrofluid or water would result in loss of barrier performance or strength.

4.3.2. Magnetic Effects on Miscibility

To test the hypothesis that ferrofluid miscibility is a function of the external magnetic field, a small vial was filled with FF1 ferrofluid to a depth of 1 cm. The vial was subsequently placed on the 5 stacked PM1 magnets. 1.0 cm of distilled water was then added to the top of the ferrofluid. No mixing was observed, and two distinct liquid layers were visible in the vial (Figure 8C). The bottom layer consisted of pure ferrofluid and the top layer was pure water. No mixing between the two the layers was observed after 30 days. An identically-prepared vial not subjected to a magnetic field showed immediate mixing of the ferrofluid and the water. After 30 days, the system remained fully mixed, and the concentration of ferrofluid was determined by the HACH spectrometer to be uniform throughout the liquid.

4.4. MAGNETOPRESSURE

The apparatus used for magnetopressure measurements consists of a horizontal column of ferrofluid connected at one end to a differential pressure transducer (DPT), with the other end

open to the atmosphere (Figure 9). The ferrofluid column in this experiment had a length of 0.12 m, with an inside diameter of 0.95 cm. To avoid magnetic effects on its metallic and electronic components, the DPT was connected to the column by means of a flexible nylon tube filled with Dow Corning 200 fluid silicone oil (Dow Corning Corporation, Midland, MI), which served as a pressure-transfer liquid. The silicone-filled tube was 1.3 m long and had an inner diameter of 0.18 cm. To cover the range of the magnetopressures measured in this experiment, three different transducers were used: Validyne DPT models DP 15-30, DP 15-26, and DP 15-20 (Validyne Systems, Northridge, CA). The transducers were calibrated with known hydrostatic pressures in a vertical water column. The DPT measurements were recorded electronically using a computer with a Validyne signal conditioning unit operated by a GPIB interface with a LabView™ (National Instruments, Austin, TX) data acquisition program.

Pressure measurements were recorded as the permanent magnets approached the end of the column connected to the pressure transducer. The 5 stacked PM 1 magnets and the PM 2 magnet (Table 3) were used in this experiment. The center of the ferrofluid column was aligned with the axis of the magnetic pole. Figures 10 and 11 show the measured magnetopressures, p_G (gage pressures), in horizontal columns filled with the FF1 and FF2 fluids, respectively.

As Moridis and Oldenburg (1998) indicated, the magnitude of the magnetopressure (p_G) and the distance over which it is effectively exerted increases with the strength and gradient of the magnetic field, and the saturation magnetization of the fluid. The dependence of p_G on the magnetic field can be seen in Figure 10, which shows the p_G exerted by in the FF2 fluid due to the 5 stacked PM1 magnets and the PM2 magnet. Figure 10 shows a rapid decline in pressure as the magnetic field strength decreases with increasing distance from the pole. The pressures created

by the 5 PM1 magnets are larger because of the stronger field strength, due to a higher B_r value

and a longer magnet length (see equation (8) and Table 3).

The increase in the p_G with an increase in the fluid magnetization is shown in Figure 11,

where the p_G created by the 5 stacked PM1 magnets in the FF2 fluid is higher than the one

created in the FF1 fluid. Although the magnetite particles are identical in the two liquids, the

larger concentration of magnetite in the FF2 creates a greater force in the fluid. The close-range

measurements in Figures 10 and 11 (i.e., the ones in the immediate vicinity of the pole) include a

certain level of uncertainty because the high field strength near the surface of the magnet causes

the ferrofluid to spike or separate from the bulk of the fluid on the interface with the silicon oil at

the end of the tube, which in turn affects the pressure measured by the transducer.

The measured magnetopressures can be compared to predicted values, utilizing the

magnetization curve of FF1 and the measured field strength of the permanent magnets.

Neglecting capillary pressures, the pressure produced in the ferrofluid can be calculated using the

ferrohydrodynamic Bernoulli equation in the following form

$$\Delta p = \mu_{mo} \overline{M} H. \tag{9}$$

Equation 9 was used along with the magnetization curve (Figure 1) and the measured magnetic

field data to calculate the magnetopressure. The results are shown in Figures 10 and 11 along

with the measured data. The fit between measurements and predictions is generally good. Some

deviation can be expected due to the difficulty of placing the tube directly in the centerline of the

large magnet and also due to the formation of spikes (Rosensweig, 1985) at the ferrofluid-silicone

oil interface at high magnetic field strength.

Moridis and Oldenburg (1998) developed the following analytical equation to predict magnetopressure, i.e., the pressure developed in a ferrofluid due entirely to the effects of an external magnetic field,

$$p_G = -\rho \frac{u_1}{u_2} \exp[-u_2(x + L_o)] \tag{10}$$

where p_G is the gauge magnetopressure (Pa), ρ is the ferrofluid density, and x is the distance from the magnetic pole. The terms u_1 and u_2 are parameters describing the magnetic effects, and incorporate all the ferrofluid magnetic properties and the geometric effects of the magnetic field distribution. An alternative equation

$$g_m(x)\frac{\partial H(x)}{\partial s} = \frac{\mu_{m0}}{\rho} M(x)\frac{\partial H(x)}{\partial x} \cong u_1 \exp(-u_2 x) \tag{11}$$

permits calculation of g_m, the magnetogravity (Moridis and Oldenburg, 1998), a term which allows the formulation of the magnetic effects of an external field on the ferrofluid in a manner analogous to gravitational effects. The u_1 and u_2 parameters for the PM1 and the PM2 magnets and the FF1 and FF2 ferrofluids are shown in Table 4.

The validity of equation (10) was confirmed from laboratory experiments. In this section we use equation (10) to evaluate the effects of very strong magnetic fields on the performance of ferrofluids. More specifically, we determine whether exposure to strong magnetic fields has any residual effects on the ferrofluids.

In this experiment we used the weaker PM2 magnet, and the FF1 ferrofluid. Figure 12 shows p_G using ferrofluid not previously exposed to a magnetic field (referred to as 'new' ferrofluid), and (b) ferrofluid previously used to determine the p_G in the very strong magnetic field created by the 5 stacked PM1 magnets ('old' ferrofluid). It can be seen that the p_G curve for

18

the new FF1 is good agreement with the theoretical prediction. The p_G for the old FF1 follows the shape of the predicted curve, but is consistently lower than that for the new fluid. This indicates that the approximation of equation (11) is valid but the values of u_1 and u_2 are different. A curve fitting of the measured p_G for the old fluid yields an excellent agreement for $u_1 = -137.553$ N/kg and $u_2 = 74.1538$, which are measurably different than the corresponding values in Table 4.

Because the magnetic field created by the permanent magnet is invariant, the changes are attributed entirely to changes in the magnetic properties of the ferrofluid. The discrepancy appears to indicate that exposure to a strong magnetic field has a residual effect on the ferrofluid magnetic behavior (e.g., due to partial particle agglomeration). Experimental studies to determine whether this adverse effect is temporary and/or reversible are currently in progress (Moridis et al., 1998).

4.5. FLOW IN HORIZONTAL HELE-SHAW CELLS

The use of Hele-Shaw cells, i.e., parallel glass plates with a narrow gap, as experimental analogues for porous media is well documented. A significant advantage of Hele-Shaw cells over 2-D porous media systems is the ability to visualize the flow. It should be noted, however, that caution should be exercised in the use of Hele-Shaw cells for the flow visualization of ferrofluids and in the interpretation of the observation. The permeability k of a Hele-Shaw cell is given as (Lamb, 1945; Saffman and Taylor, 1958)

$$k = \frac{a^2}{12} \tag{12}$$

where a is the gap width.

In the following experiments, ferrofluid was injected into water-filled, horizontal Hele-Shaw cells and the ferrofluid movement under the influence of a magnetic field was monitored. Due to different wettability characteristics (caused by the significantly lower surface tension of ferrofluids because of the presence of stabilizing surfactants), equation (12) might not be entirely applicable. Moreover, if the cell gap is filled with a liquid (such as water) with a density significantly less than the ferrofluid, gravitational separation may occur, with the ferrofluid sinking to the bottom of the cell. Finally, because the miscibility of a water-based ferrofluid is inhibited by the presence of a magnetic field, the liquids between the cell plates cannot be considered homogeneous, behave as a two-phase system, in which solubility is controlled by the magnetic field.

4.5.1 Experiment HS1

A schematic of the Hele-Shaw cell used in the experiments is shown in Figure 13. The Hele-Shaw cell was constructed from two 0.25 m x 0.28 m glass plates (plate thickness = 6.4 mm). A 1.6 mm shim was placed around the edge and between the plates, the edges of the plates were sealed with silicone caulk, and the cell gap was filled with water. Based on the volume of water necessary to fill the cell, we concluded that the average gap width was 2 mm, which was due to either expansion of the cell gap by the emplaced water or from a non-planer surface of the glass. Using equation (12), this gap width will produce an estimated permeability, k, in the Hele-Shaw cell of 3×10^{-7} m^2.

The plates were leveled horizontally, and 0.3 ml of FF1 ferrofluid was injected using a 20-gauge syringe needle (see Figure 13). Following the injection, the syringe was removed and an external magnetic field was applied using the 5 stacked PM1 magnets. The cell gap was centered on the pole face of the magnet, aligned with y-z plane of the pole face at $x = 0$ (see Figure 2).

The magnetic field gradient attracted the ferrofluid moved toward the magnet and the movement was recorded utilizing a time-indexed CCD video camera. A series of images captured from the video of Experiment HS1 is shown in Figure 14. Plate (a) shows the initial ferrofluid shape before the application of the external magnetic field. At 219 s, the fluid has moved to form the teardrop shape shown in plate (b). As the teardrop elongates, the fluid closest to the magnet accelerates because in encounters higher magnetic field strength and a steeper field gradient. In plate (c) at 277 s, the fluid acceleration is sufficiently large to result in small-scale turbulent instabilities, which appear as fingers in the advancing ferrofluid front. In plate (d) at 427 s, the fluid has reached the sealed end of the Hele-Shaw cell and is accumulating symmetrically around the magnet. The fluid continues migrating until the bulk of the fluid accumulates against the magnet forming a symmetric, arc-shaped pool.

Despite the complete water miscibility of FF1, mixing with the water in the cell gap appears to be very limited. When mixing occurs, it is indicated by a lighter-gray halo around the ferrofluid. The determination of the dilution of ferrofluid by direct observation is difficult due to the opacity of the fluid even at low concentrations. In the magnetic segregation experiments described previously, even a 1:100 dilution of ferrofluid was visually indistinguishable from the pure ferrofluid. The segregation experiments, however, demonstrated that any mixing, especially in the presence of a magnetic field, is limited and reversible. This is attributed to the strong

attractive forces between the ferrofluid and the magnet, and the resulting magnetically-controlled miscibility. When the ferrofluid particles are aligned with the magnetic field, free Brownian motion is inhibited and mixing is limited.

Of particular interest is that the fluid, regardless of the pathway to the magnet, accumulates invariably in a symmetric, arc-shaped pool. This predictable and reproducible shape has potentially important implications in environmental applications. For example, a series of injections followed by magnetic attraction periods could be used to accumulate a ferrofluid with a reactant or barrier liquid against a magnet, thus covering the target zone by a series of overlapping fluid spheres.

4.5.2 Experiment HS2

The flow of ferrofluid in the Hele-Shaw cell in Experiment HS1 was slower than that predicted from the estimated permeability of $k = 3 \times 10^{-7} \text{ m}^2$ calculated from equation (12) for an average gap width of 2 mm. The higher density and viscosity of FF1 can account for the slower rate, although some of these effects could be counter-balanced by the lower surface tension of the ferrofluid. From the size of the disk formed in the initial injection of the ferrofluid into the Hele-Shaw cell and the known volume of fluid injection, the initial thickness of the ferrofluid in Experiment HS1 (Figure 14, plate a) was estimated to be 0.067 mm, or 1/30th of the gap width. This indicated that the fluid had spread in a thin layer on the bottom plate due to the higher density of the ferrofluid (specific gravity 1.2). The estimated permeability experienced by the ferrofluid based on the smaller gap width is calculated to be $4 \times 10^{-8} \text{ m}^2$ using equation (12). However, in this experiment the FF1 fluid only contacts the lower plate while the top surface

interacts with the water in the cell gap. The effect of the water-ferrofluid interaction on the permeability of the cell is unknown.

To achieve a more realistic Hele-Shaw analogy of ferrofluid flow in a porous medium, it was desirable for the ferrofluid to contact both glass plates. To achieve this, a second experiment was performed, in which the water in the cell gap was replaced with colloidal silica (Nyacol 5880, EKA Nobel, Marietta, GA). This water-based material is completely miscible with ferrofluid and has a similar specific gravity and density (specific gravity = 1.16, μ = 0.0004 Pa·s). Because of the better match to the ferrofluid properties, the ferrofluid does not sink to the bottom but fills the whole cell gap. The effective permeability of the cell is thus expected to be larger than in the HS1 experiment, and equal to the theoretical estimate of 3 x 10^{-7} m^2 (if possible wettability effects are neglected).

The captured video images of Experiment HS2 (Figure 15) show the flow of ferrofluid in a colloidal silica-filled Hele-Shaw cell with a 2 mm gap width (calculated based on the injection volume). The captured video images (a), (b), (c), and (d) in Figure 15, have corresponding times of 0, 22, 85, and 114 seconds. The overall pattern of movement is similar to the flow in experiment HS1 (Figure 14), though the higher permeability of this system and better property match between liquids resulted in higher velocities and more unstable flow, evidenced by the more pronounced bifurcations and turbulence of the leading edge of the advancing ferrofluid front.

4.5.3. Experiment HS3

The Hele-Shaw analogy used above is applicable to laminar flow regimes. In experiments HS1 and HS3, the flow was initially laminar. However, as the ferrofluid experienced high

magnetic fields and steep field gradients, turbulent instabilities were observed. These turbulent eddies would not form in the subsurface because of the much lower flow velocities due to the close packing of the porous media.

To achieve a flow that more closely simulates porous media flow, a third experiment was conducted in which a cell was fabricated with one smooth glass plate and one rough, "shower-door" type glass plate (3/16 inch, P516 obscure glass, UC Glass company, Berkeley, California).

The size of this cell was 0.22 m x 0.33 m. Two 30-gauge needles were inserted into the gap to facilitate filling the gap with liquid. The plates were sealed with silicone at the edges, placed in an aluminum frame, and compressed while the silicone was drying. This ensured contacts (asperity contacts) between the rough and smooth plates at a number of locations. The roughness of the P516 shower glass precluded estimating the Hele-Shaw cell permeability by equation (12).

The cell was filled with Nyacol 5880 colloidal silica through one of the 30-gauge needles. Complete saturation could not be achieved in the time-frame of this experiment, and some small air bubbles remained in the cell gap. The plates were leveled horizontally, with the rough plate on the bottom to ensure that the ferrofluid, which has a slightly higher density than the colloidal silica, would contact the rough plates throughout the flow. A volume of 0.5 ml of FF2 ferrofluid was injected through one of the syringe needles and the 5 stacked PM 1 magnets were placed at the far corner of the opposite end from the injection point.

The movement of the ferrofluid through the cell in Experiment HS3 is captured in Figure 16. The four images (a), (b), (c), and (d) correspond to 0 s, 348 s, 586 s, and 836 s, respectively. The flow pattern of the ferrofluid as it advances toward the magnet is similar to that observed in

24

the smooth glass plates in the previous two experiments. The observed bifurcations in the flow are due to splitting of the advancing fingers as they encounter entrapped air bubbles, and are not thought to be due to turbulent flow. Because of lower permeability, the velocity was lower and the turbulent bifurcations of the previous experiments were not observed. The general flow regime and the accumulation pattern in the vicinity of the magnet are the same as observed in the smooth plate flows of Experiments HS1 and HS2.

4.5.4 Experiment HS4: Flow in a vertical Hele-Shaw cell

To investigate the interaction of gravity and magnetic force in ferrofluid flow, a smooth-glass Hele-Shaw cell with a gap width of 1 mm and dimensions of 0.25 m x 0.25 m was oriented vertically and filled with water (see Figure 17). Three edges of the cell were sealed with silicone, and the top edge was left open to the atmosphere. The 5 stacked PM1 magnets were placed alongside the cell, 0.15 m from the cell bottom, with the pole of the magnet oriented with the center of the gap.

FF2 ferrofluid was injected into the water in the cell 0.01 m below the cell top. At a distance of 0.17 m from the magnet (position 1, Figure 17), magnetic attraction overcame gravity and all of the ferrofluid accumulated next to the magnet. At a distance of 0.20 m (position 2) the competition between gravity and magnetic attraction is more balanced: the majority of the fluid accumulated near the magnet, with a portion falling under gravity to the bottom of the cell as the magnetic field did not have sufficient time to act on it. At a distance of 0.22 m (position 3), the magnetic field is weak, and all of the injected fluid fell to the bottom of the cell. Over time, the ferrofluid formed a static arc-shaped pool around the magnet. The shape of the accumulation of

the ferrofluid around the magnet is the practically identical to that observed in the horizontal cells. Of particular importance is the observation that, regardless of the orientation of the plates, the symmetric arc-shaped pool is still formed around the magnet.

4.6. FLOW IN HORIZONTAL 2D POROUS MEDIA DOMAINS

The movement of ferrofluids through porous media was investigated in shallow beds of the saturated S2 sand (K, hydraulic conductivity, $= 4.2 \times 10^{-2}$ cm/s, $\phi = 0.46$) in trays with dimensions of 0.1 m x 0.12 m. The thickness of the sand bed was 1 cm. After saturating the sand-filled trays with water, the sand surface was smoothed and was left exposed. Ferrofluid was injected into the sand to form an initial ferrofluid distribution that was approximately circular or band-shaped across the width of the tray. An external field was then applied using the 5 stacked PM1 magnets. The ferrofluid movement through the sand was recorded using a video camera which was activated and time-indexed at appropriate intervals.

4.6.1. Circular distribution

Typical results of a sand-bed experiment with an initial circular ferrofluid distribution are shown in Figure 18. In image (a), 0.5 ml of FF2 ferrofluid was injected into the sand tray at a distance of 0.1 m from one side of the tray. The magnet was then placed at the edge of the tray (the right side in the image) so that the center of the sand was on the y-z plane of the magnetic pole at $x = 0$. Images (b) and (c) depict the ferrofluid distribution at 23 and 43 minutes after injection. The flow of fluid toward the magnet is very similar to that observed in the Hele-Shaw

experiments without sand. The ferrofluid initially follows a direct pathway toward the center of the magnet. As the ferrofluid reaches the end of the tray, the magnet causes the ferrofluid to pool in a semi-circle.

4.6.2. Band distribution

The movement of ferrofluid from an initial band-shaped distribution is shown in Figure 19. 1.0 ml of FF1 was injected into the water-saturated S2 tray at 0.1 m from the edge of the plate. The magnet was oriented as described in section 4.6.1, and the movement was recorded as the ferrofluid moved through the sand. The images, a, b, c, and d in Figure 19 are at times 0, 2.77, 2.87, and 21 hours, respectively.

In Figure 19b, several fingers of fluid (probably corresponding to the highest permeability pathways) break from the band and move toward the magnet. Figure 19C shows the fingers traveling to the magnet. As in the Hele-Shaw cell, the fluid accelerates as it approached the magnet, due to the higher magnetic field and steeper field gradient. Once a continuous path to the magnet is established, accumulation of the fluid begins and the final ferrofluid distribution is very similar to that in the experiment with the circular initial ferrofluid distribution. The difference in the size of the final ferrofluid pool in the two experiments reflects the larger amount of ferrofluid in the band.

Experiments with larger sand trays duplicated the same pattern of movement from distances of 0.25 m when the 5 stacked PM1 magnets (Figure 20) were used. As the distance from the magnet increased, the initial ferrofluid velocity decreased. To cover the distance of 0.25 m through the saturated sand to the magnet takes on the order of 1 week. As in the Hele-Shaw

experiments, the process of deformation of the initial disk to a tear drop shape takes up most of this time. As previously observed, the velocity increases as the fluid approaches the magnet, due to the increasing magnetic field strength and field gradient.

4.6.3. Flow in vertical 2-D porous medium

An experiment in a vertical cell, filled with S3 sand, was conducted to observe the interaction of magnetic field and gravity in the flow of a ferrofluid in porous media. The ferrofluid was injected 20 cm from the magnet. As in the vertical Hele-Shaw experiment HS4, the ferrofluid experiences both gravitational and magnetic forces as it migrates downward. In this case, the slower movement allows more time for magnetic forces to have an effect. Magnetic forces dominate and the end point accumulation is the familiar semi-circular pool, with a slight but discernible asymmetry due to the presence of gravity (see Figure 21).

5. Discussion

The aim of the experiments presented here was to investigate the potential for controlling the emplacement of liquid in the subsurface through control of the external magnetic field. The experiments demonstrated that magnetic forces cause ferrofluid to flow over distances of order 0.25 m on time scales of hours to days. The forces generated can be quite large, rivaling those of gravity for density differences of the order of 200 kg/m^3. Furthermore, after being mobilized by magnetic forces, ferrofluids are held at steady state in a static and predictable arc-shaped configuration around the magnet.

These experimental observations have important implications for using ferrofluids for emplacement of viscous liquid barriers, treatment chemicals, and imagable tracers in the subsurface. For example, one possible application involves placing columns of magnets in boreholes around an isolation or treatment zone. Subsequent injection of ferrofluids with appropriate carrier liquids (barrier or reactants) would result in migration and accumulation against of liquid around the permanent magnets, creating a predictable and reproducible final structure. This process may be repeated to ensure complete coverage of a treatment area, or to produce overlapping barrier layers. Such barriers could be used for landfills or to seal leaking tanks or pipes. Another use would be to emplace ferrofluid, which by virtue of its high electrical conductivity and magnetic permeability, exerts a strong geophysical signal, for use as an imagable tracer. Imagable tracers could be used to image the fracture zone, or for barrier verification where leaks would be detectable through geophysical surveys that locate ferrofluid.

Several important issues arise when considering the applicability of ferrofluids for subsurface fluid emplacement: (1) length scales; (2) dilution; (3) interaction with porous media and (4) stabilization with novel carrier liquids.

The most important issue concerns the length scales over which magnetic forces can be generated. The fact is that magnetic field strength (H) declines rapidly with distance from the magnet. Since the force is proportional to the gradient of the magnetic field strength as well as the magnetization (M) which is a strong function of H at low H, there is an even more rapid decline in force with distance from the magnet. Nevertheless, the experiments presented here demonstrate that ferrofluid can be mobilized by permanent magnets over length scales of order 0.25 m. And very near the magnet, magnetic forces can be quite large as observed in Figure 21

where the arc-shaped pool around the magnet is hardly affected by gravity even through the density difference is of order 200 kg/m^3. In general, we expect mobilization of ferrofluid over length scales greater than 1 m will be impractical, although superconducting electromagnets offer some hope of using stronger magnets to increase this length scale. Nevertheless, the strong attraction of ferrofluid to magnets over shorter length scales may be useful in subsurface applications, as discussed above, and can find immediate use in laboratory experiments where it is necessary to manipulate fluid in an apparatus without physically contacting the liquid.

The second issue we discuss is that of dilution. Specifically, ferrofluid will mix with groundwater in the subsurface by advection, dispersion, and molecular diffusion. Adsorption or magnetic attraction of ferrofluid onto solid grains may dilute it further in groundwater. These processes will be augmented by the observed tendency of ferrofluid to be pulled in differing directions by gravitational and magnetic forces as it is attracted toward a permanent magnet. This tendency arises from the fact that ferrofluid closer to the magnet experiences significantly larger forces per unit volume than ferrofluid farther away. Thus an initially circular pool such as that in Figure 14 will be deformed and elongated. At the extreme are situations such as that in Figure 17 where part of the ferrofluid is pulled toward the magnet and part is pulled downward by gravity. Once ferrofluid is diluted, the strength of the magnetic body force on the mixture decreases and the ability to control emplacement is impaired. While some of these effects have been investigated in this paper, clearly more work is necessary to evaluate the importance of dilution in field applications.

The third issue is the interaction of ferrofluid with the porous media. Significant potential effects include filtration and reactions that could destabilize the ferrofluid. Our experiments to

date show that sand has no adverse effects either through filtration or reaction, but we have yet to test fully a wide range of soil types. Any processes that can influence the magnetite-surfactant bond, including the effect of variations in the pore water chemistry, the change in ferrofluid particle size with dilution, bacterial action, and the strength of the magnetic field could irreversibly change the ferrofluid. This change could cause flocculation and sedimentation of the ferrofluid. This area should be the next area of experimental study.

The fourth issue is that of stabilization of the ferrofluid with carrier liquids such as viscous liquid barriers and other subsurface reactants. To date, ferrofluids have been stabilized with a variety of mineral oils, water, and organic solvents (Berkovsky, 1996). Other carrier liquids to be considered will have to be evaluated on a per case basis and will require further study.

6. Conclusions

The above observations have important implications for using ferrofluids for emplacement of viscous liquid barriers and treatment chemicals in the subsurface. Columns of magnets could be placed in boreholes around an isolation or treatment zone. Subsequent injection of ferrofluids with appropriate carrier liquid (barrier or reactants) would result in movement in response to the magnetic field and accumulation against the permanent magnets, creating a predictable and reproducible final structure. This process may be repeated to insure complete coverage of a treatment area, or to produce overlapping barrier layers.

The experiments described here were designed to evaluate the potential for controlling the emplacement of ferrofluid in porous media. The multitude of observations in this study can be summarized by four main conclusions:

(1) Permanent magnets create a predictable pressure gradient in a magnetic fluid;

(2) Ferrofluid can be driven through porous media to consistent and predictable final configurations, which are controlled solely by the magnetic field and are unaffected by the flow pathway, permeability, or initial injection shape;

(3) Ferrofluid does not show any evidence of filtration or loss of ferrofluid particle strength as it flow through sand;

(4) Investigations indicated that under the influence of a magnetic field, ferrofluids demonstrate magnetically controlled miscibility, and segregation after dilution.

These conclusions support the further investigation into the use of ferrofluids to aid in the precise emplacement of fluids in the subsurface. To make the use of ferrofluids for emplacement effective, the ferrofluid would have to be stabilized in the desired carrier liquid. This carrier liquid could contain reactants or barrier liquids for *in situ* treatment. In addition to fluid development, magnetic fields created by grids of permanent magnets would have to be designed to drive the fluids.

The magnetic segregation and solubility experiments showed that addition of water had no significant effect on ferrofluid stability. The resistance to mixing of the magnetized ferrofluid with surrounding liquids can be exploited in regions where precise placement of treatment chemicals is necessary. For example, injection of effective but potentially toxic treatment chemicals would

become feasible because the risk of migration is low. Prior to implementation, more study on the stabilization of different chemicals with ferrofluid would be needed. Any processes that can influence the magnetite-surfactant bond, including the effect of variations in the pore water chemistry, the change in ferrofluid particle size with dilution, bacterial action, and the strength of the magnetic field could irreversible change the ferrofluid. This change could causes flocculation and sedimentation of the ferrofluid or a permanent change in the water content of the fluid. A limitation observed in these experiments is that the field of influence of permanent magnets decreases rapidly with distance. This limitation will have be considered in any design of a magnetically controlled fluid emplacement system.

The development of this technology would provide a valuable tool in controlling liquids in the subsurface. The ferrofluids would be especially useful in situations where precise placement is paramount, or if excavation or pump and treatment methods are not possible due to high toxicity.

7. Acknowledgments

8. References

Berkovsky, B.M.: *Magnetic Fluids and Applications Handbook,* Begell House, Inc., New York, 1996.

Berkovsky, B.M., Medvedev, V.F., Krakov, M.S.: *Magnetic Fluids, Engineering Applications.* Oxford University Press, Oxford, 1993.

Chorney, A.F., and Mraz, W.: Hermetic sealing with magnetic fluids, *Machine Design,* **5** (1992) 79-82.

Dieulin, J.: 1982. Filtration de colloides d'actinides par une colonne de sable argileux. *Report LHM/RD/82/83.* Paris School of Mines, Fontainebleau.

Herzig, J.P., Leclerc, D.M. and Le Goff, P.: Flow of suspension through porous media, *Ind. Eng. Chem.* **62**(5) (1970), 129-157.

Ives, K.J.: Deep Bed Filter. *Mathematical Models and Design Methods in Solid-Liquid Separation.* A. Rushton, ed. Martinuj Nijohoff, Dordrecht, 1975, pp. 90-149.

Lamb, H: *Hydrodynamics,* Dover, New York, 1945.

Lerk, C.F, and P.M. Heertjes.: The functioning of deep bed filters, Part II, the filtration of flocculated suspensions. *Transactions,* Institute of Chemical Engineers, Vol. 45 (1967). p. T138.

McCaig, M. and Clegg, A.G.: *Permanent magnets in theory and practice.* 2nd ed., John Wiley and Sons, New York, 1987.

Moridis, G.J., Borglin, S.E., Oldenburg, C.M., and Becker, A.: *Theoretical and experimental investigations of ferrofluids for guiding and detecting liquids in the subsurface.* Lawrence Berkeley National Laboratory Report LBNL-41069, Berkeley, California, March, 1998.

Moridis, G.J., and Oldenburg, C.M.: *Ferrofluid Flow in Porous Media.* Lawrence Berkeley National Laboratory Report LBNL-41486, Berkeley, California, March, 1998.

Nunes, A.C. and Yu, Z.C.: Fractionation of a water-based Ferrofluid, *J. of Magnetism and Magnetic Materials.* **65** (1987), 265-268.

Oldenburg, C.M., Borglin, S.E., and Moridis, G.J.: *Numerical simulation of ferrofluid flow for subsurface environmental engineering applications.* submitted to *Transport in Porous Media,*

also Lawrence Berkeley National Laboratory Report LBNL-40146, Berkeley, California, June, 1998.

Raj, K and Moskowitz, R: Commercial applications of ferrofluid, *J. of Magnetism and Magnetic Materials.* **85** (1990), 233-245.

Rosensweig, R.E.: *Ferrohydrodynamics.* Cambridge University Press, Cambridge, 1985.

Saffman, P.G., and Taylor, G.I.: The penetration of a fluid into a porous medium or Hele-Shaw cell containing a more viscous liquid. *Proc. Roy Soc. London Ser. A,* **245** (1958) 312-29.

Schroth, M.H., S.J. Ahearn, J.S. Selker, and J.D. Istok. Characterization of Miller-Similar Silica Sands for Laboratory Hydrologic Studies. *J. Soil Sci. Soc. Am.* **60** (1996) 1331-1339.

Table 1. Physical Properties of EMG 805^{TM} (FF1) and EMG-C^{TM} (FF2) ferrofluid (Ferrofluidics Corporation, Nashua, NH).

Property	EMG 805^{TM} (FF1)	EMG-C^{TM} (FF2)
Viscosity, μ, at 27°C	0.0025 Pa·s	0.008 Pa·s
Magnetite Concentration	3.7 %	5.2 %
Surfactant Concentration	8 %	10 %
Water Concentration	88.3 %	84.8 %
Initial Magnetic Susceptibility	6.16 (MKS units)	6.16 (MKS units)
pH	7	7
Density	1190 kg/m^3	2000 kg/m^3
Saturation Magnetization	1.6 x 10^4 A/m	3.1 x 10^4 A/m

Table 2. Physical Properties of Monterey #60 sand, OK-1 silica sand, Unimin 30/40 mesh sand, and NTS Soil

Soil	Designation	Porosity, φ	Hydraulic Conductivity, K, (m/s)	D_{10} (m)
NTS	S1	0.22	1.8 x 10^{-6}	4.6 x 10^{-5}
Monterey #60	S2	0.46	4.2 x 10^{-5}	2.2 x 10^{-4}
Unimin 30/40 mesh	S3	0.33	1.5 x 10^{-3} (Schroth et al., 1996)	0.45 x 10^{-3} (Schroth et al., 1996)
OK-1	S4	0.34	3.6 x 10^{-6}	6.5 x 10^{-5}

Table 3. Properties of the NdFeB Magnets.

Magnet Type	Description	Field Parameters	Dimensions
NdFeB (PM1)	Permanent magnet, Rectangular shape	$B_r = 1.2$ T $H_c = 1.0 \times 10^5$ A/m	$L_o = 0.0254$ m $2a = 0.05$ m $2b = 0.05$ m
NdFeB (PM2)	Permanent magnet, Rectangular shape	$B_r = 1.1$ T $H_c = 0.93 \times 10^5$ A/m	$L_o = 0.0254$ m $2a = 0.035$ m $2b = 0.035$ m

Table 4. u_1 and u_2 values for Equations (10) and (11).

Magnet + Ferrofluid	u_1 (N/kg)	u_2 (N/kg)
PM1 + FF1	-368.25	55.124
PM1 + FF2	-422.87	55.124
PM2 + FF1	-426.16	96.477
PM2 + FF2	-489.38	96.477
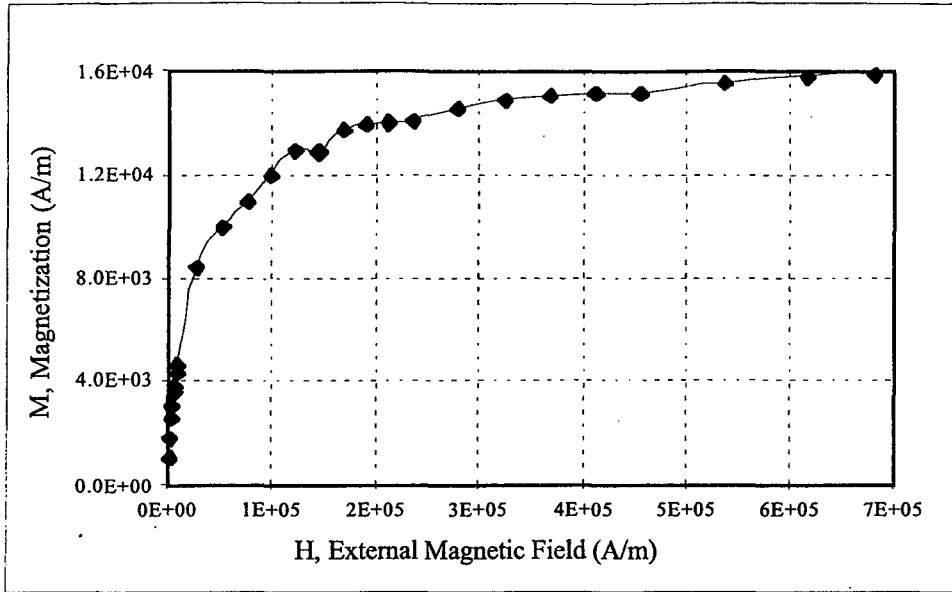
Figure 1. Magnetization Curve for EMG 805™ (FF1 ferrofluid) (Nunes and Yu, 1987)
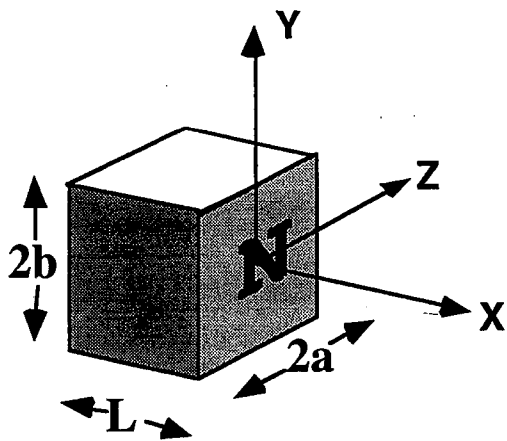
Figure 2. Permanent Magnet Configuration
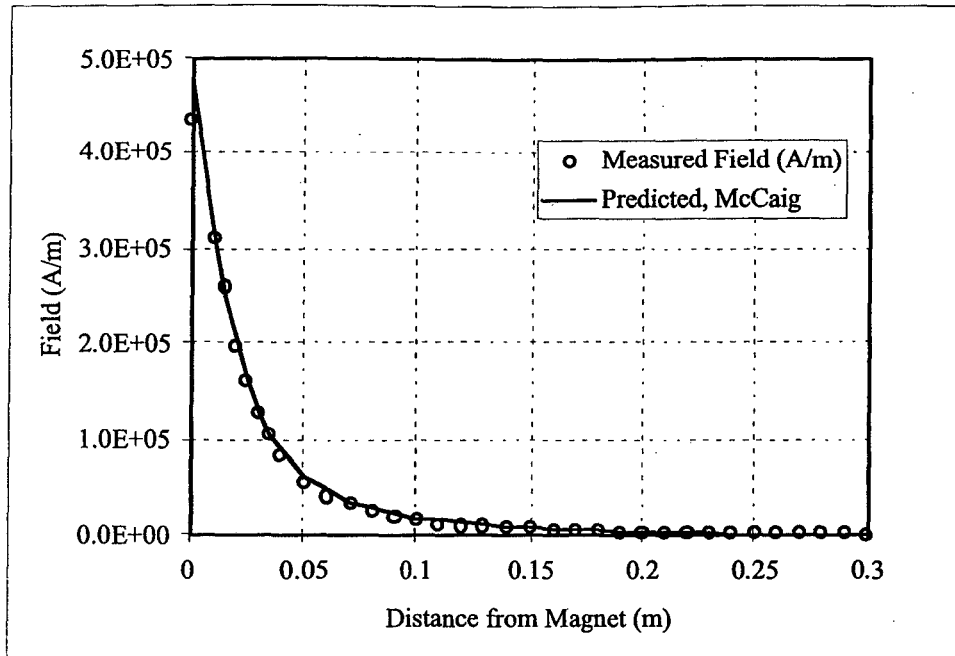
Figure 3. Predicted and measured magnetic field from 5 stacked PM1 magnets. Dimensions of the magnet and parameters of magnet strength are given in Table 3.
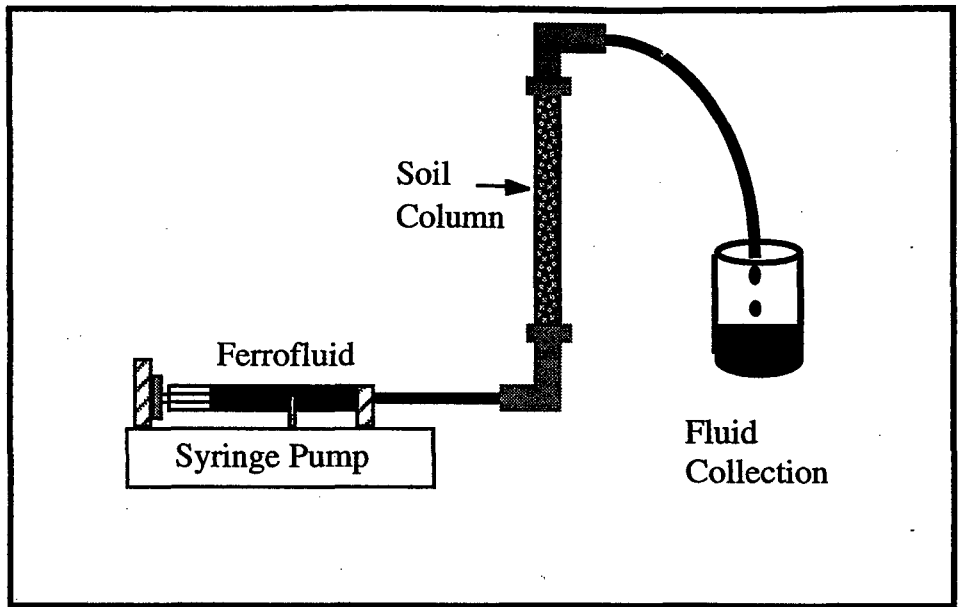
Figure 4. Schematic of ferrofluid filtration testing apparatus
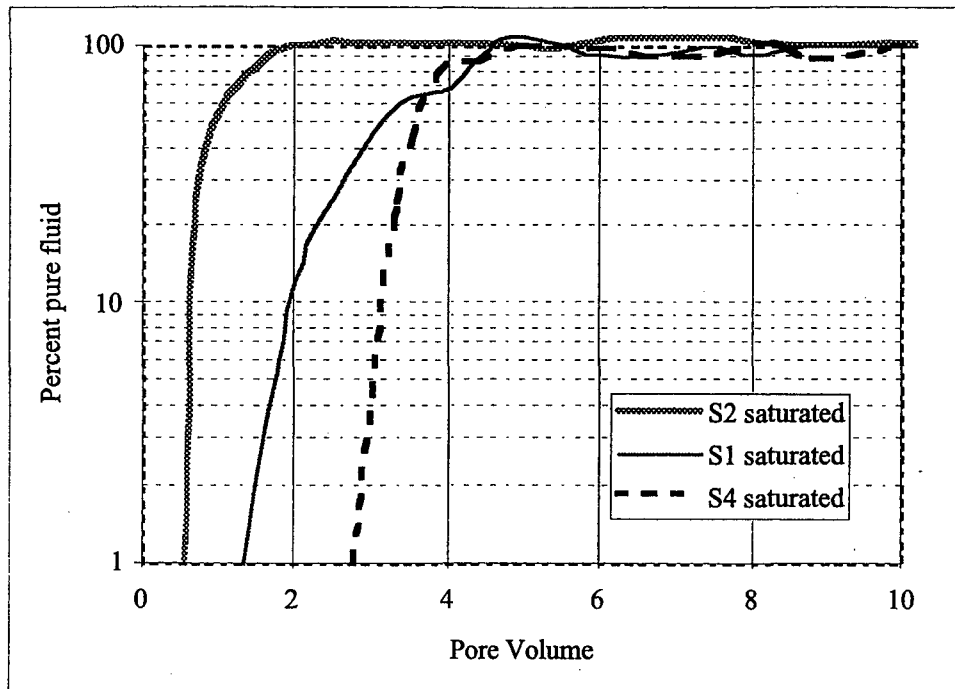
Figure 5. Concentration of FF1 ferrofluid eluted through saturated sand columns.
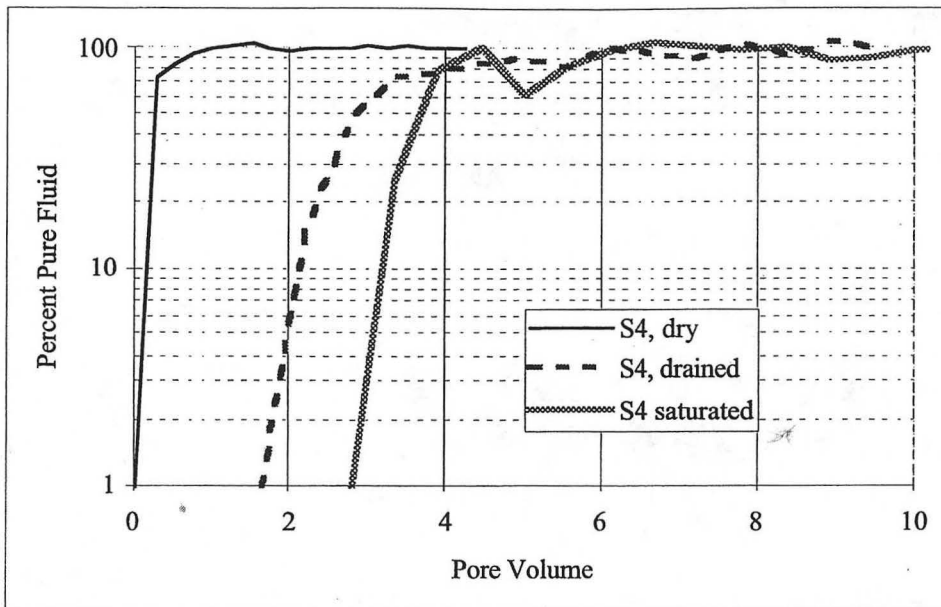
Figure 6. FF1 ferrofluid concentration eluting from sand columns containing dry, partially water-saturated, and water-saturated OK-1 (S4) sand.
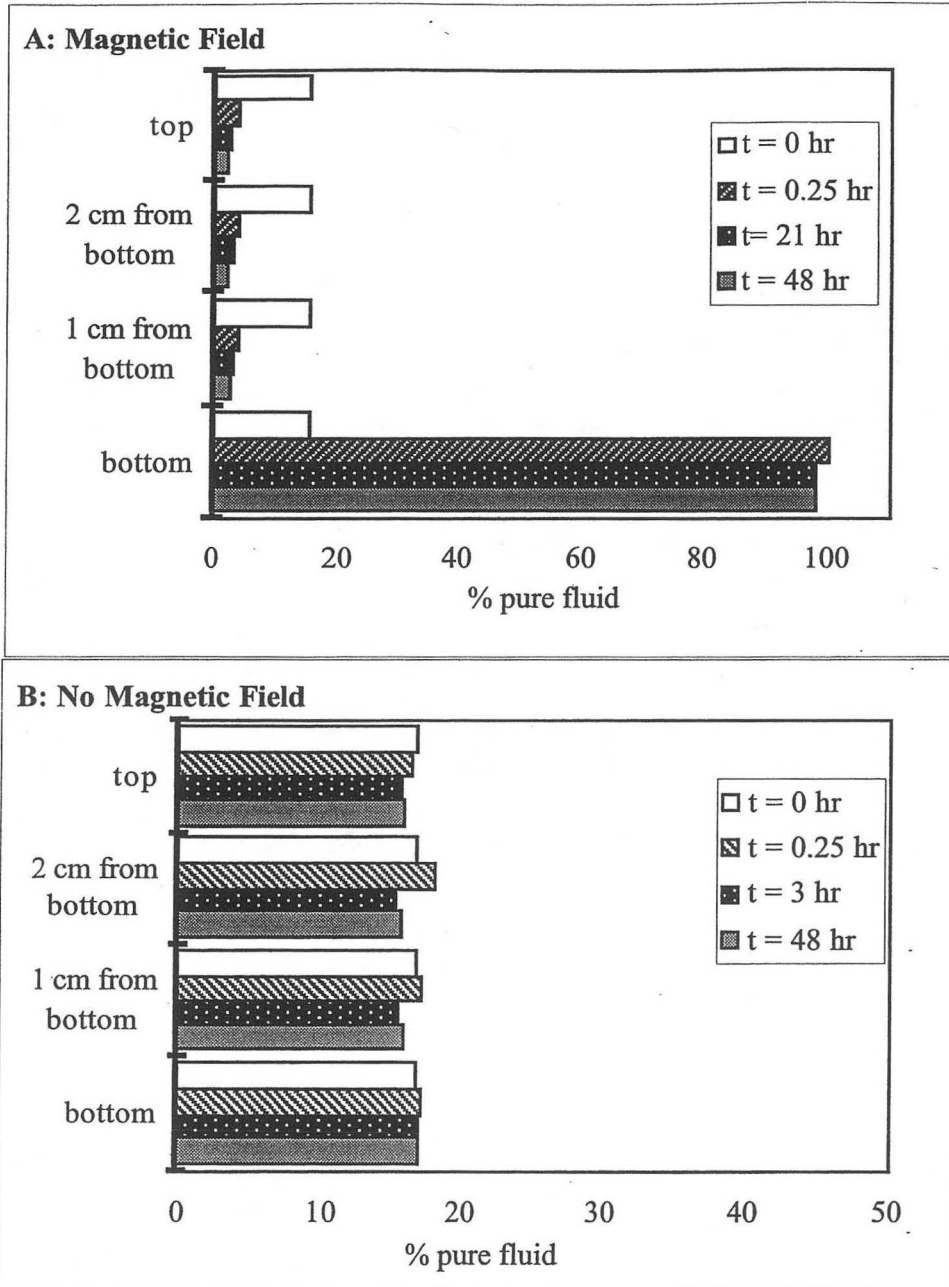
Figure 7. Concentration of diluted FF1 ferrofluid. In Plot A the diluted FF1 ferrofluid is on five stacked PM1 magnets, in Plot B there is no magnetic field present.
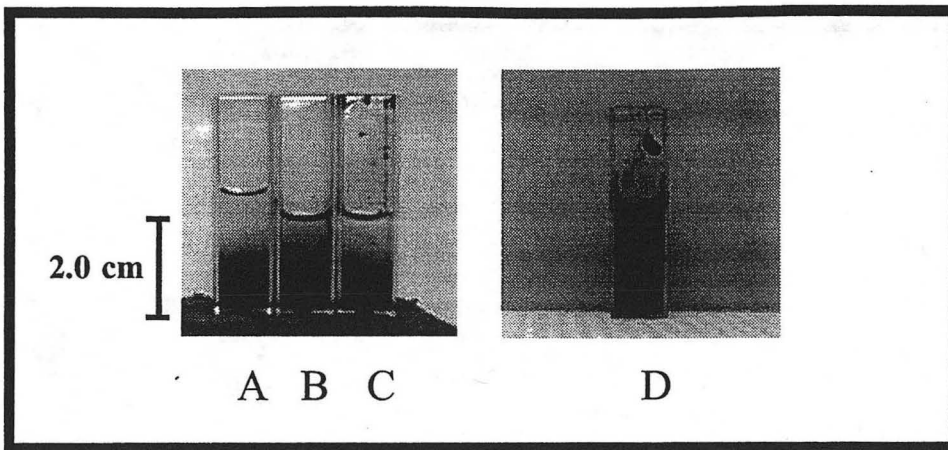
Figure 8. Separation of diluted FF1 ferrofluid by the 5 stacked PM1 magnets after 30 days. Vials A and B contain 1:2 and 1:1 dilution of FF1 ferrofluid, respectively, and were initially mixed prior to placement in the magnetic field. Vial C contains a 1:1 dilution of ferrofluid, and was prepared by adding clean water above magnetized FF1 ferrofluid. Vial D contains a 1:1 dilution of ferrofluid which was initially mixed. Vial D was not subjected to a magnetic field and shows no separation after 30 days.
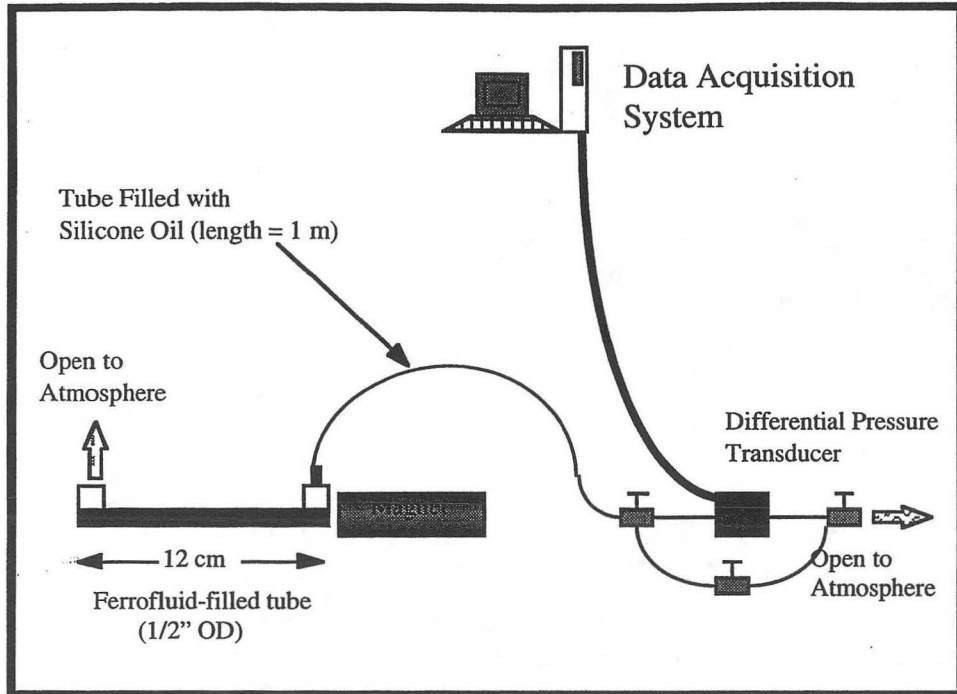
Figure 9. Schematic of magnetopressure measurement apparatus
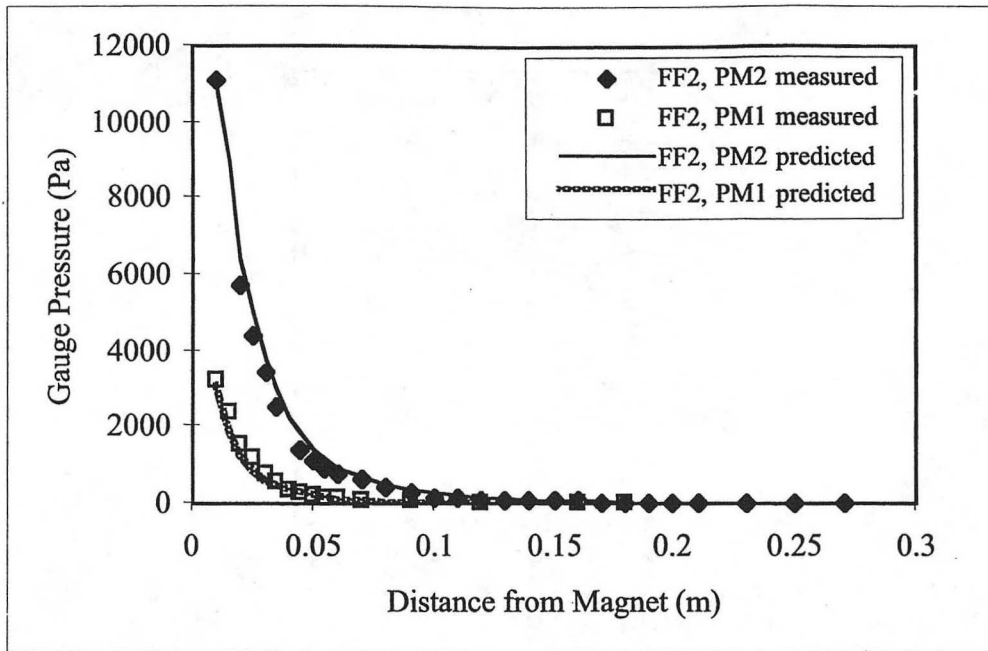
Figure 10. Measured and predicted pressures for FF2 (EMG-C^TM) ferrofluid using the five stacked PM1 magnets and the PM2 magnet.
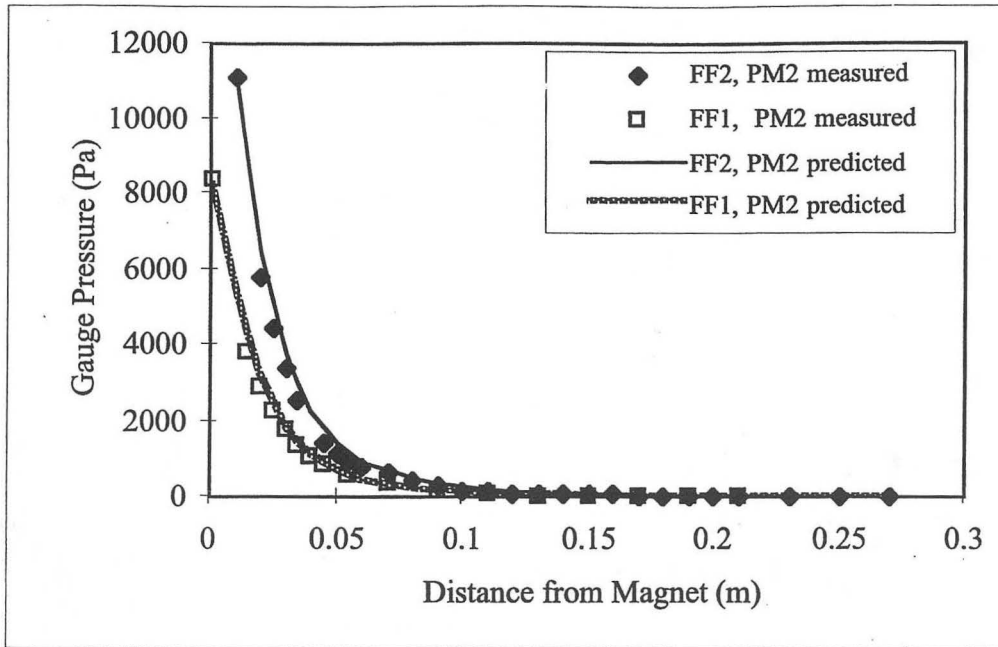
Figure 11. Measured and predicted pressures for FF2 (EMG-C^{TM}) and FF1 (EMG 805^{TM}) ferrofluids using the five stacked PM1 magnets.
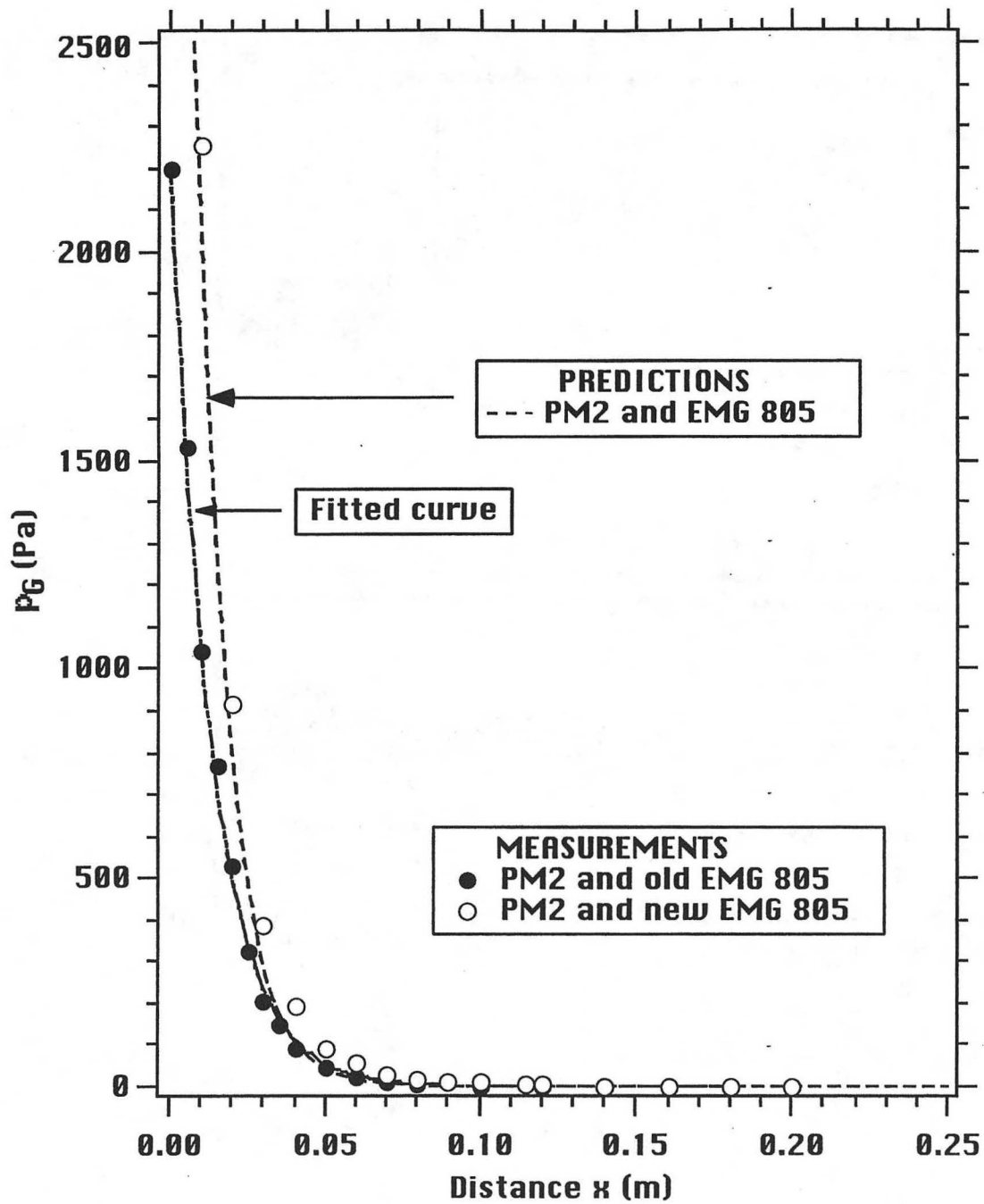
Figure 12. p_G for FF1 (EMG 805[TM]) previously unexposed to magnetic field ('new' fluid) and for FF1 previously exposed to magnetic field ('old' fluid). The curve for the new fluid fits well with the predicted values for p_G (Moridis and Oldenburg, 1998). To match the pressure measurements for the old fluid, the values of u_1 and u_2 were fitted to adjust to the different magnetic properties of the old FF1 fluid.
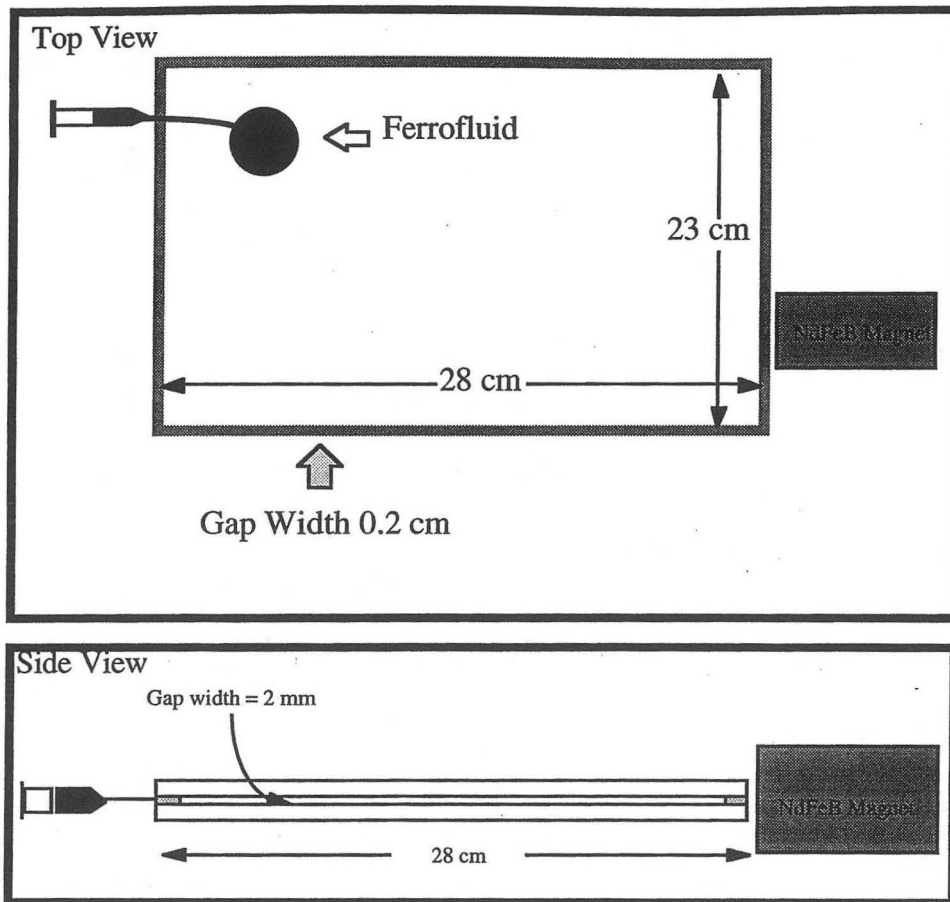
Figure 13. Top and side views of a typical horizontal Hele-Shaw cell used to observe ferrofluid movement. The position of the magnet and the injection point shown in the top view varies according to experiment.
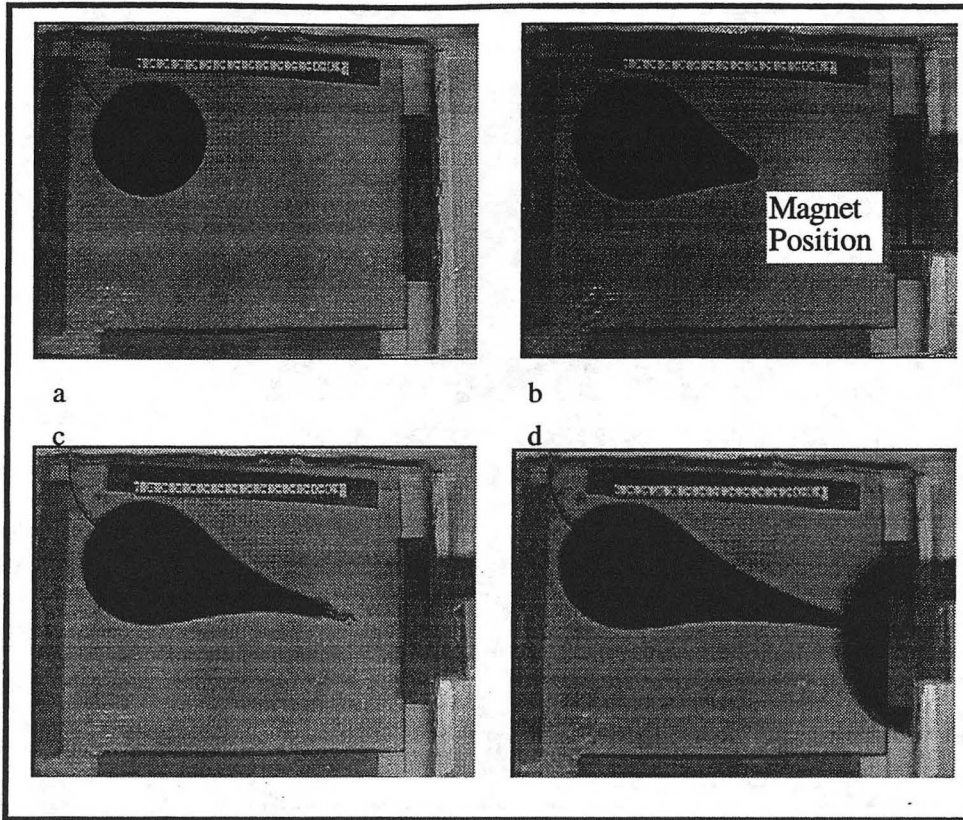
Figure 14. Experiment HS1. Progression of FF1 ferrofluid through water- filled horizontal Hele-Shaw cell. The magnetic field was produced by five stacked PM1 magnets. Frames a, b, c, and d are at times 0, 219, 277, and 427 seconds, respectively.
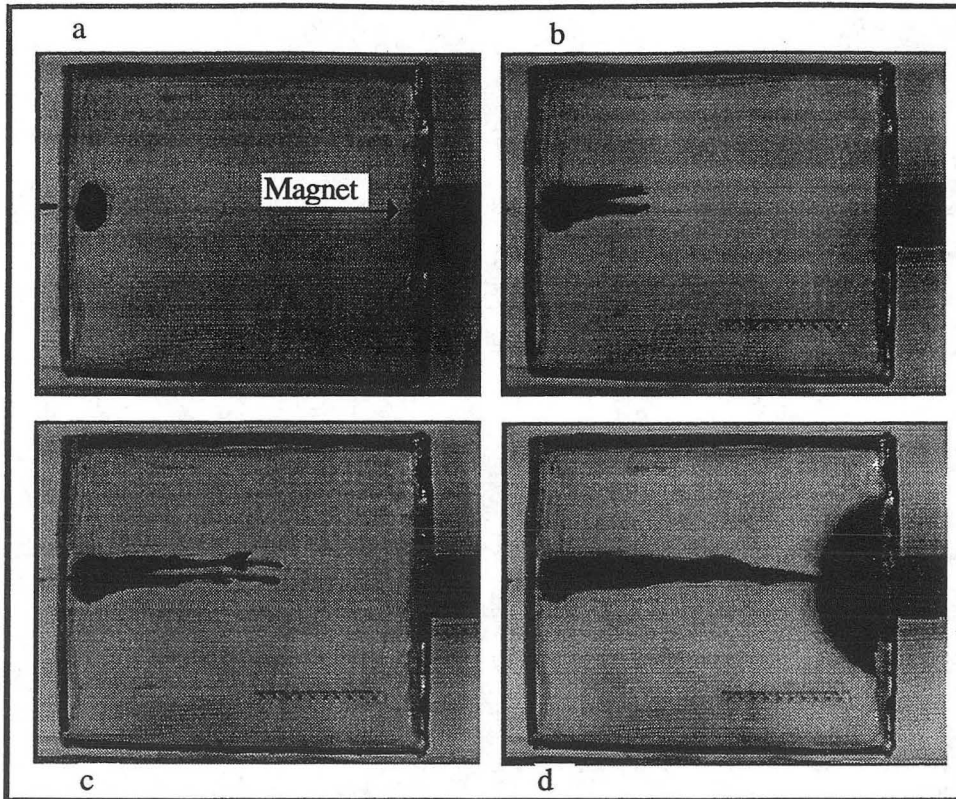
Figure 15. Experiment HS2. Progression of FF1 ferrofluid through Hele-Shaw cell filled with Nyacol 5880 colloidal silica. The magnetic field was provided by five stacked PM1 magnets. Frames are at times (left to right, top to bottom) 0, 22, 84, and 114 seconds.
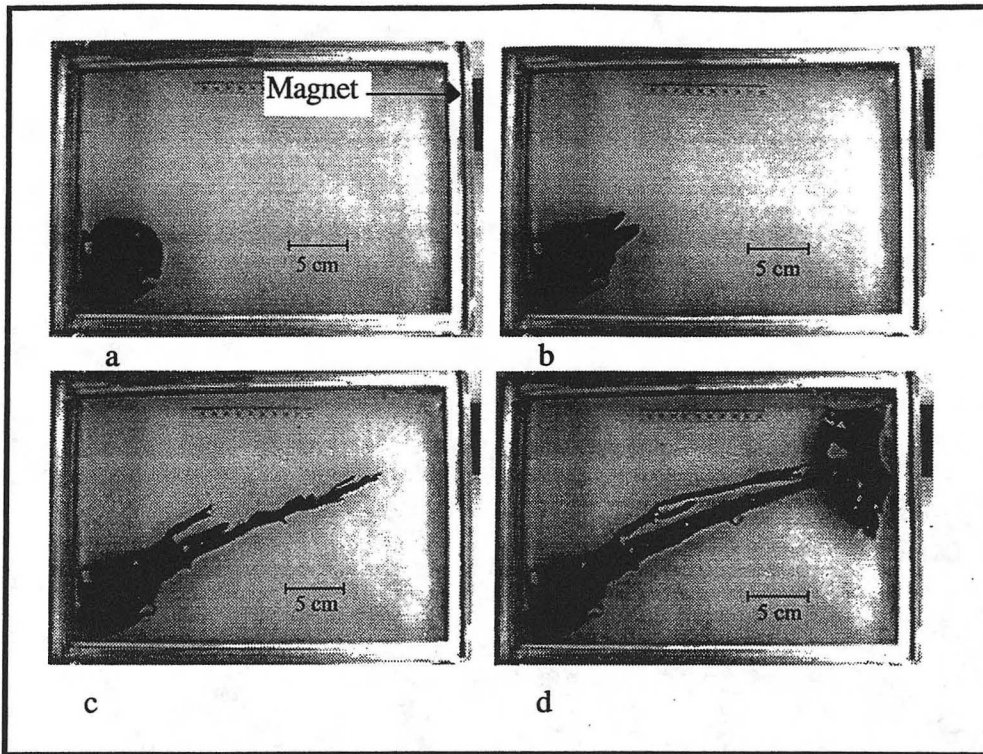
Figure 16. Experiment HS3. Progression of FF1 ferrofluid through a Hele-Shaw cell constructed of a lower P516 rough shower door glass plate and an upper smooth glass plate. Cell filled with Nyacol 5880 Colloidal Silica. Frames are taken at 0, 348, 586, and 836 seconds, respectively. The magnetic field was produced by 5 stacked PM1 magnets.
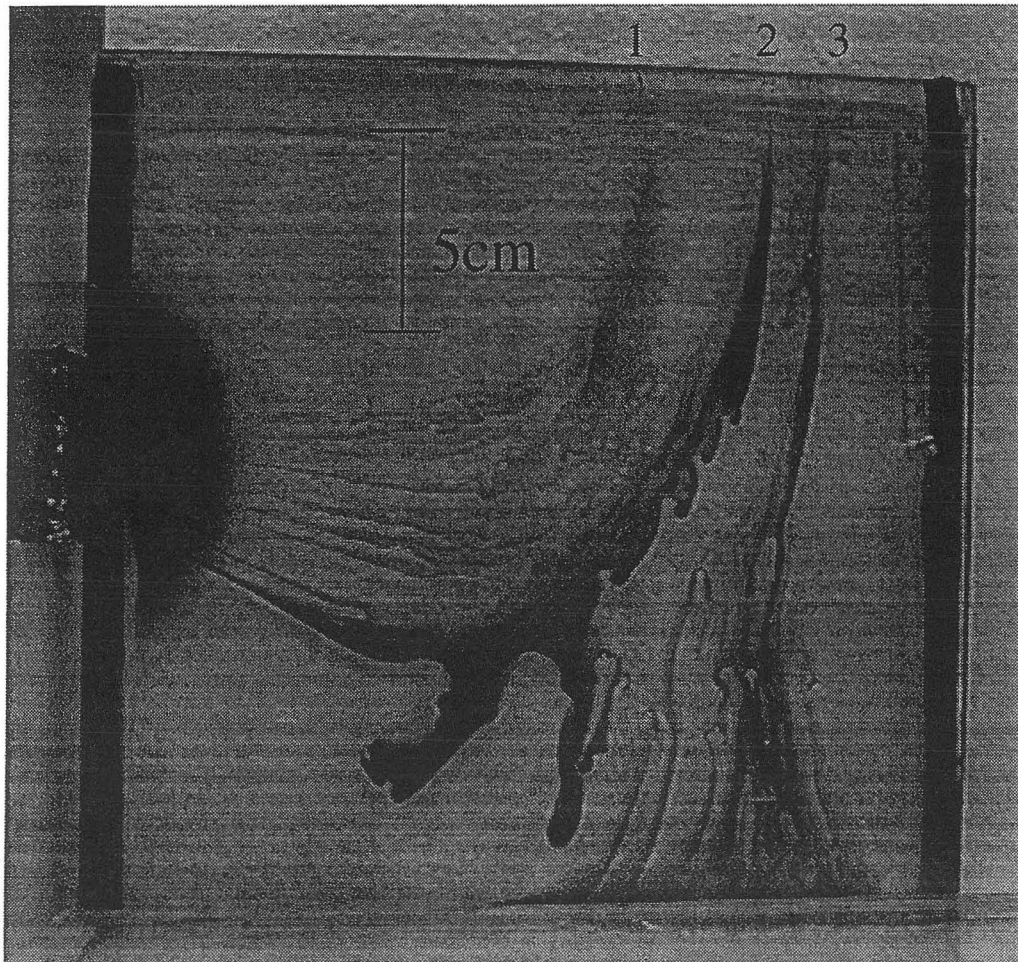
Figure 17. Experiment HS 4. Movement of FF1 ferrofluid through a vertical Hele-Shaw cell. Five stacked PM1 magnets are located at the left side of the frame. Three injection points are shown in the figure: (1) 17 cm from magnet, showing 100 % travel to magnet, (2) 20 cm from the magnet showing partial travel to magnet, partial fall under gravity, and (3) 22 cm showing 100 % fall to bottom.
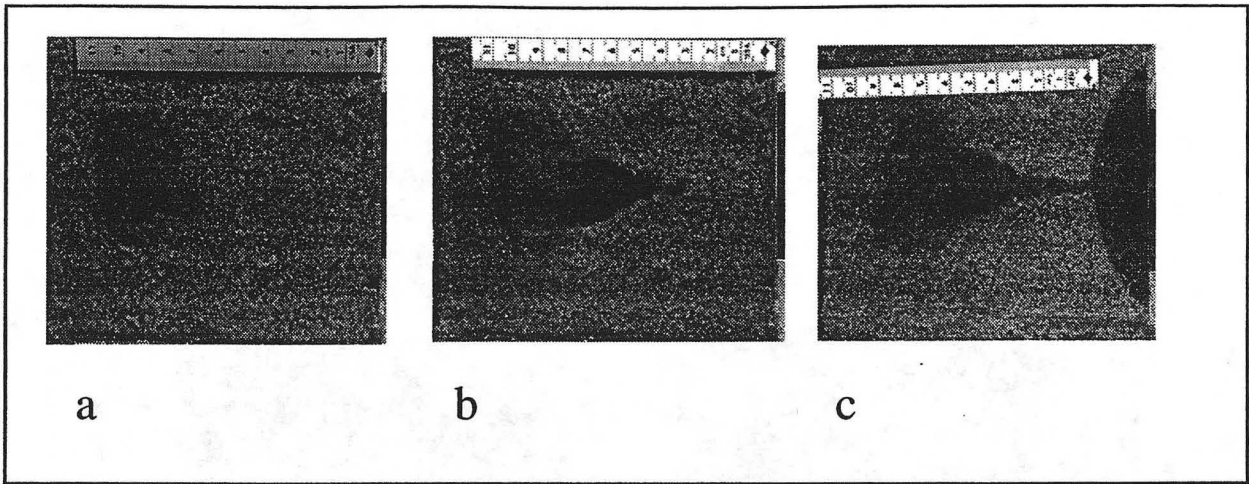
Figure 18. Movement of FF2 ferrofluid with an initial circular injection through water-saturated Monterey #60 sand. Frames are at 0, 23, and 43 minutes.
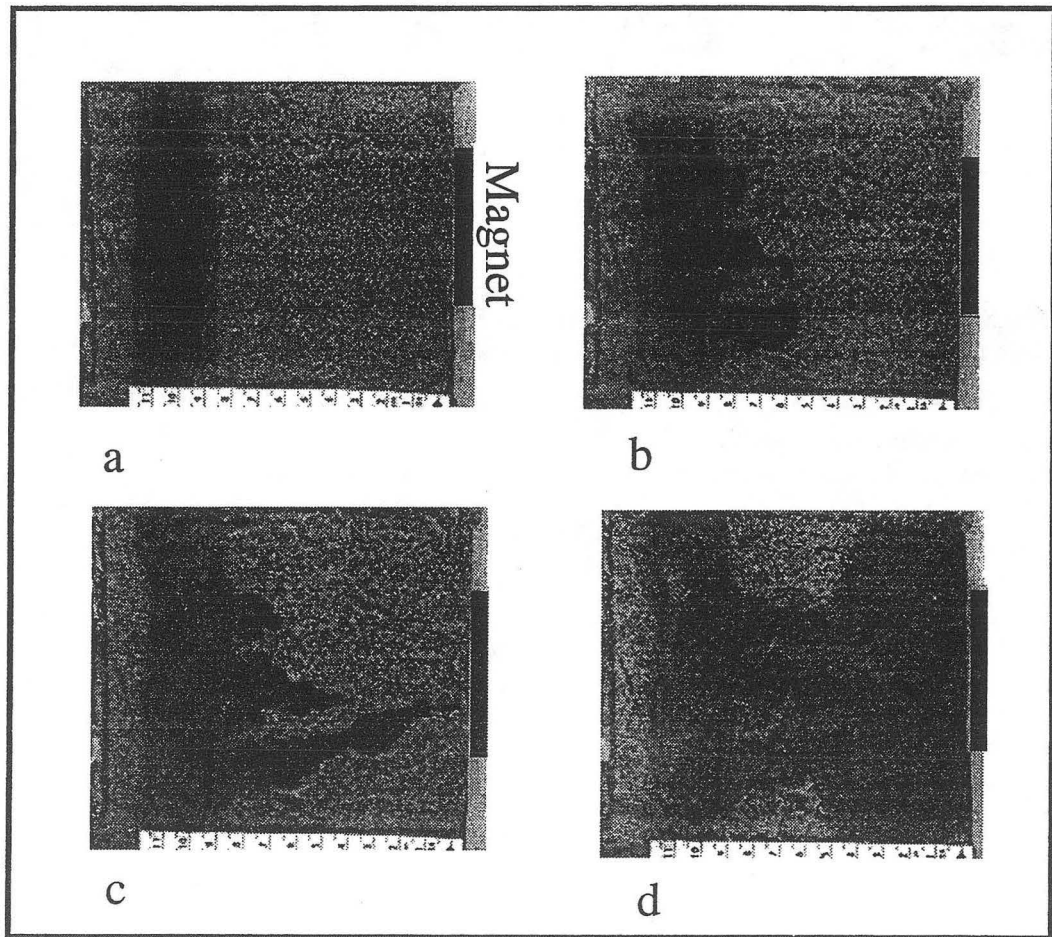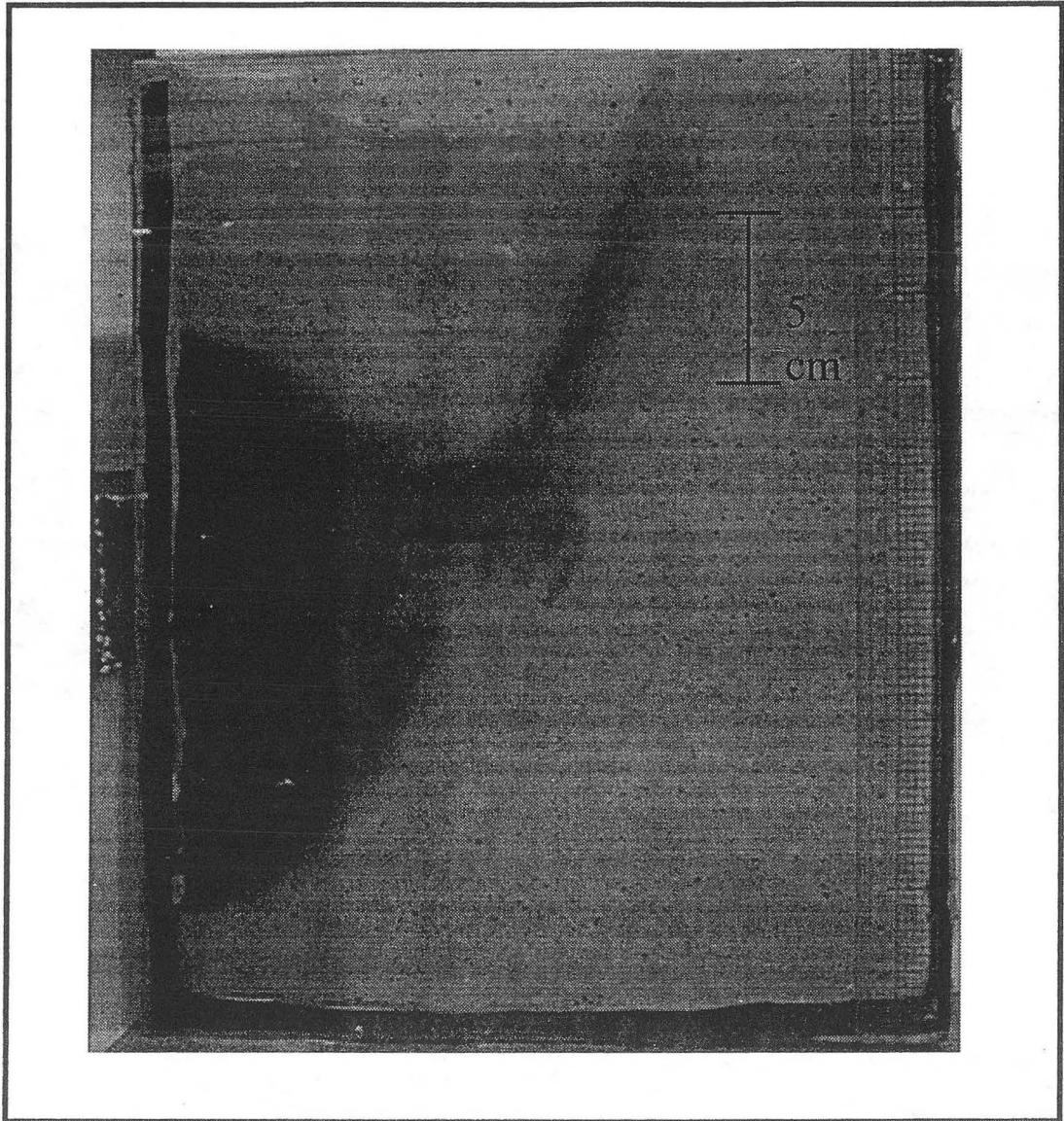
Figure 19. Movement of FF2 ferrofluid with an initial band-shaped injection through water-saturated S1 sand. Times are 0, 2.77, 2.87, and 21 hours.
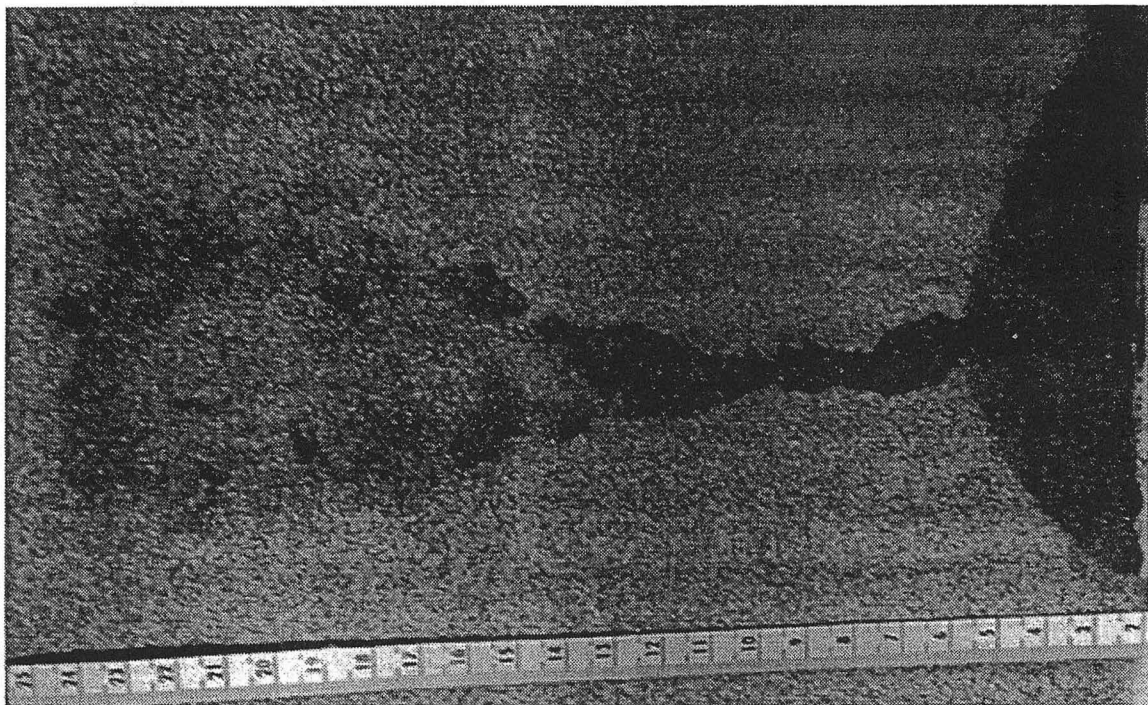
Figure 20. FF2 ferrofluid movement through water-saturated S1 sand. Five stacked PM1 magnets are located on the center of the right side of the tray. Initial ferrofluid injection into the sand was circular at a distance of 0.25 m from the face of the magnet. The figure shows the system seven days after initial injection.

Figure 21. Movement of FF2 ferrofluid through a vertically oriented cell filled with S2 sand. Magnet is located in the center of the left side. Time elapsed is 75 minutes.